Spin Orbit Interactions in Nuclear Matter with Auxiliary Field Diffusion Monte Carlo

by

Jie Zhang

A Dissertation Presented in Partial Fulfillment
of the Requirement for the Degree
Doctor of Philosophy

Approved November 2014 by the
Graduate Supervisory Committee:

Kevin Schmidt, Chair
Ricardo Alarcon
Richard Lebed
John Shumway

ARIZONA STATE UNIVERSITY

December 2014

ABSTRACT

Spin-orbit interactions are important in determining nuclear structure. They lead to a shift in the energy levels in the nuclear shell model, which could explain the sequence of magic numbers in nuclei. Also in nucleon-nucleon scattering, the large nucleon polarization observed perpendicular to the plane of scattering needs to be explained by adding the spin-orbit interactions in the potential. Their effects change the equation of state and other properties of nuclear matter. Therefore, the simulation of spin-orbit interactions is necessary in nuclear matter.

The auxiliary field diffusion Monte Carlo is an effective and accurate method for calculating the ground state and low-lying exited states in nuclei and nuclear matter. It has successfully employed the Argonne v6' two-body potential to calculate the equation of state in nuclear matter, and has been applied to light nuclei with reasonable agreement with experimental results. However, the spin-orbit interactions were not included in the previous simulations, because the isospin-dependent spin-orbit potential is difficult in the quantum Monte Carlo method. This work develops a new method using extra auxiliary fields to break up the interactions between nucleons, so that the spin-orbit interaction with isospin can be included in the Hamiltonian, and ground-state energy and other properties can be obtained.

ACKNOWLEDGEMENTS

I would like to thank my advisor Professor Kevin Schmidt for all his help during my Ph.D. I learned a lot from this project. I could not do this work without his advising and support.

When I was in high school, I enjoyed the feeling of 'I knew I was right when I was right' while solving Physics problems. But in college, I didn't study one objective from different ways for complicated problems. The self-checking feeling comes back when Professor Schmidt suggested me to use different ways to double check a new result which hasn't been calculated yet. I like this way to do research. Sometimes I knew what should be done logically, but didn't know how to make progress. I really appreciate Professor Schmidt's great ideas and patience to show me the correct way. After years of Ph.D. research, I learned not only Physics and algorithms, but also how to do research. I used to think life is long, so there is plenty of time to do research. But now I think Life is an integral of time, and the integrand needs to be optimized.

I also would like to thank Professor Ricardo Alarcon, Professor Richard Lebed, and Professor John Shumway. I really appreciate their help and advice. Professor Alarcon helped me a lot when I was a TA. Professor Lebed gave me useful suggestions on my plan of study. I would like to especially thank Professor Shumway for attending my defense via video. It is a big favor. Professor Shumway used to organize 'Theory group meeting' for graduate students, from which I enjoyed and learned a lot.

Last, I would like to thank National Science Foundation under grant PHY1067777 for support.

TABLE OF CONTENTS

CHAPTER Page

LIST OF TABLES

LIST OF FIGURES

Chapter 1

INTRODUCTION

1.1 Background

Nuclear interactions between protons and neutrons play an important role in nuclear matter studies, such as nuclei structure and neutron star structure [1][2][3]. The study of nuclei structure[4] shows that the stable nuclei lie along the magic numbers line, and could be explained well by shell model[5]. There are many nuclei far from stability. They are usually not found on the earth, but make a big contribution to the universe. These unstable nuclei with large neutron excess could decay back to the stable nuclei, and the boundary of instability where extra neutrons are no longer bound is called the neutron drip line[6]. These neutron-rich nuclei have many more neutrons than protons, so the boundary force is very weak. This makes their half-life very short and hard or impossible to determine in experiments[7]. Similarly, a large ratio of neutrons over protons exists in neutron stars. We can learn some internal properties of neutron stars by observing the neutrinos[8], but the matter inside neutron stars is very difficult to reach by present observations. By solving the Schrödinger equation using realistic 2- and 3-body interactions[9] in neutron matter, we can predict the equation of state and the mass density inside neutron stars[10]. Therefore, the simulations of the Schrödinger equation using realistic interactions is very important in nuclear physics.

Among kinds of ab initio methods for nuclear structures[11], Quantum Chromodynamics (QCD) could present a fundamental approach via lattice[12], but QCD calculations can only be applied to limited number of nucleons. To date, only limited

data on the two-body interaction has been predicted. For low-energy nuclear interactions, phenomenological potentials are typically employed for accurate calculations such as the Faddeev-Yakubovsky equation for A=4[13], variational calculations for the Schrödinger equation in A=6 nuclei[14][15], etc. Those potentials are in non-relativistic quantum system, so they are only dependent on positions and spinors of nucleons. The phenomenological potentials are obtained by fitting experimental scattering data, and can describe light nuclei very well [16][17][18][19][20].

In recent decades, many theoretical nuclear calculations have used phenomenological potentials to calculate the equation of state of nuclear matter. Green's function Monte Carlo[21][22] gives an accurate result for neutron matter [23][24][25] and nuclei[26], but can only be applied to systems with the number of nucleons up to A=12, for systems with protons and neutrons, and A=14 for pure neutron systems. The no-core shell model can extend the number of nucleons up to A=40, but it needs a truncated basis and soft potentials. The Fermi hypernetted chain method is based on integral-equation techniques, but it makes uncontrolled approximations, and the variational ansatz used is limited by the integral equation methods. We use auxiliary field diffusion Monte Carlo[27][28][29] because it is efficient and can be applied to larger nuclei than the Green's function Monte Carlo. When the number of nucleons increases, the auxiliary field diffusion Monte Carlo scales polynomially in the particle number, which is much better than the exponential scaling in the Green's function Monte Carlo. Also, the simulation results of auxiliary field Monte Carlo for light nuclei agree with the Green's function Monte Carlo results very well when the same interactions are used.

Auxiliary field diffusion Monte Carlo has been successfully applied to a phenomenological potential called Argonne v6' with nuclear matter[30]. However, the spin-orbit interactions[31][32][33][34] were dropped. The spin-orbit interactions are

very important in giving the correct energy level orderings in the shell model of nuclei. They are the interactions between total spin of two nucleons and relative orbital angular momentum of two nucleons. Deep inside of nuclei, the spin-orbit interactions of a single nucleon might be partially cancelled by two nucleons with spins in opposite directions. But at the surface, there are spin-orbit interactions for a single nucleon since there is no cancellation. These interactions make the energy levels split and lead to the magic numbers of nuclei. Also in nucleon-nucleon scattering, the large nucleon polarizations observed perpendicular to the plane of scattering[35] needs to be explained by adding the spin-orbit in the potentials. Therefore, to fully understand the structures of nuclear matter[36][37], it's necessary to include spin-orbit interactions in the phenomenological potentials.

The spin-orbit interactions have been estimated by some other theoretical methods like chiral effective field theory[34]. In chiral perturbation theory, the spin-orbit strength was generated by iterated one-pion exchange at saturation density [38][39], and agreed with the empirical value used in the shell model. In this work, we are going to evaluate the spin-orbit interactions in auxiliary field diffusion Monte Carlo at zero temperature to establish a more accurate equation of state of nuclear matter. The method can then be applied to neutron-rich nuclei as well as other more stable nuclei to obtain a general method to calculate nuclear structure from a realistic nuclear Hamiltonian.

1.2 Outline

The following chapters will describe in detail how to include spin-orbit interactions in the phenomenological Hamiltonian to calculate the equation of state in nuclear

matter. The results will be compared with those from Hamiltonians without spin-orbit interactions, so that we can see clearly the differences the spin-orbit interactions make for the equation of state for high-density nuclear matter.

In chapter 2, we introduce the specific phenomenological Hamiltonian[40] we are using, and why we chose that Hamiltonian. A plot of the potential terms and the format of the operator dependence will be presented. We point out why we need to include the spin-orbit interactions in the potential. The relative importance of the spin-orbit interaction can be seen directly from figure 2.1.

In chapter 3, we introduce the auxiliary field diffusion Monte Carlo method, and describe how to use it to solve the Argonne v6' potential. The results of Argonne v6' in the auxiliary field diffusion Monte Carlo done by S. Fantoni, S. Gandolfi, F. Pederiva and K.E. Schmidt[30] are shown at the end of this chapter.

In chapter 4, we include spin-orbit interactions in our Hamiltonian for neutron and nuclear matter. The spin-orbit interaction is important in obtaining the correct nuclear structure, and difficult to simulate. In this chapter, we first show how other people have calculated the spin-orbit interaction contribution in neutron matter[41], and why it has not been included previously in nuclear matter. We then show how we add the spin-orbit interactions in our auxiliary field diffusion Monte Carlo calculation of nuclear matter.

In chapters 5 and 6, the detailed method and results with the spin-orbit interactions are presented. The spin-orbit interaction without isospin is calculated, and the equation of state is shown in chapter 5. The spin-orbit interaction with isospin has been calculated in the two-nucleon system. The results are showed in chapter 6. They are checked by the Lanczos method, which is described in Appendix A.

Chapter 2

HAMILTONIAN

The phenomenological nucleon-nucleon(NN) potential is obtained by fitting experimental scattering data. Before 1993, a variety of potential models fit a subset of the nucleon-nucleon scattering data to obtain various potentials like Argoone v4[42], Urbana v14[43], Bonn potential[44][45], Paris potential[46], Reid potential[47], etc. In 1993 the Nijmegen group analysed all np and pp scattering data below 350 MeV[48]. The potentials which fit the Nijmegen data[49] with $\chi^2/N_{data} \sim 1$ are called modern NN potentials[50].

In 1995, the Argonne group published a new NN modern potential by fitting all the Nijmegen np and pn scattering database, low-energy nn scattering parameters, and the deuteron binding energy. This potential is called Argonne v18[51]. It has been successfully applied to nuclear matter and light nuclei, and gives accurate results [52][53][54]. We will use Argonne v18 as the potential that all our interactions are based on in this work.

The Argonne v18 potential is then used in a many-body Hamiltonian with the form

$$H = \sum_i \frac{-\hbar^2}{2m_i}\nabla_i^2 + \sum_{i<j} V_{ij} + \sum_{i<j<k} V_{ijk} \tag{2.1}$$

It's a non-relativistic Hamiltonian including a kinetic energy operator, a two-body potential obtaining the corrected V_{ij} which is, or is based on, Argonne v18, and a three-body potential V_{ijk}. The three-body potential is necessary for obtaining the correct triton binding energy and the correct structure in heavier nuclei. The largest part of the three-body interaction has been included in the auxiliary field diffusion

Monte Carlo(AFDMC) method, and the remaining part can often be added perturbatively. The most important part of the Hamiltonian neglected in AFDMC is the spin-orbit interactions in the two-body potential. In later chapters, we will use the kinetic energy operator and two-body potential only to calculate the ground-state energy, and compare the results of the two-body potential with or without spin-orbit interactions. However, we will still give a brief introduction of the three-body potential at the end of this chapter. These can be turned on to give a more complete interaction.

2.1 Argonne v18 Two-Body Potential

The Argonne v18 potential is composed of an electromagnetic(EM) interaction, a one-pion-exchange(OPE), and short-range phenomenology. The OPE and short-range phenomenological parts are combined as strong interactions. Since they are much stronger than the EM part, I will discuss the OPE and short-range phenomenological parts first.

$$v_{ij} = v_{ij}^{\pi} + v_{ij}^{R}. \tag{2.2}$$

Here i, j are the nucleons, v_{ij}^{π} is the OPE potential, and v_{ij}^{R} is the short-range phenomenological potential. OPE is considered as meson exchanges between nucleons. It has a charge-dependency structure due to the difference in the charged- and neutral-pion masses. It is written as:

$$\begin{aligned} v^{\pi}(pp) &= f_{pp}^2 v_{\pi}(m_{\pi^o}), \\ v^{\pi}(np) &= f_{pp} f_{nn} v_{\pi}(m_{\pi^o}) + (-)^{T+1} 2 f_c^2 v_{\pi}(m_{\pi^{\pm}}), \\ v^{\pi}(nn) &= f_{nn}^2 v_{\pi}(m_{\pi^o}). \end{aligned} \tag{2.3}$$

The partial-waves f_{pp}, f_{nn}, and f_c are found to have very little difference, and are chosen to be a fixed value $f^2 = 0.075$ [55]. T is the isospin and

$$v_\pi(m) = (\frac{m}{m_s})^2 \frac{1}{3} mc^2 [Y_\mu(r)\vec{\sigma_i} \cdot \vec{\sigma_j} + T_\mu(r) S_{ij}], \tag{2.4}$$

where $Y_\mu(r)$ and $T_\mu(r)$ are the Yukawa and tensor functions:

$$\begin{aligned} Y_\mu(r) &= \frac{e^{-\mu r}}{\mu r}(1 - e^{-cr^2}), \\ T_\mu(r) &= (1 + \frac{3}{\mu r} + \frac{3}{(\mu r)^2})\frac{e^{-\mu r}}{\mu r}(1 - e^{-cr^2})^2, \end{aligned} \tag{2.5}$$

with $\mu = mc/\hbar$. m_s is a scaling mass to make the coupling constant dimensionless. The Gaussian factors cut off the one-pion exchange at short distances.

The short-range phenomenological part consists of central, L^2, tensor, spin-orbit, and quadratic spin-orbit terms. All the parameters in this part are fit to all the Nijmegen scattering data.

In auxiliary field diffusion Monte Carlo, we usually write the two-body potential v_{ij} in the operator form.

$$v_{ij} = \sum_{p=1,18} v_p(r_{ij}) O^p_{ij}, \tag{2.6}$$

where O^p_{ij} are the 18 operators given below, and $v_p(r_{ij})$ are the corresponding coefficients for each operator. The first eight operators are the most important. They give the most contribution on fitting S-wave and P-wave NN scattering data.

$$O^{p=1,8}_{ij} = [1, \vec{\sigma}_i \cdot \vec{\sigma}_j, S_{ij}, \vec{L} \cdot \vec{S}] \otimes [1, \vec{\tau}_i \cdot \vec{\tau}_j]. \tag{2.7}$$

S_{ij} is the tensor operator,

$$S_{ij} = 3(\vec{\sigma}_i \cdot \hat{r}_{ij})(\vec{\sigma}_j \cdot \hat{r}_{ij}) - \vec{\sigma}_i \cdot \vec{\sigma}_j, \tag{2.8}$$

$\vec{L}$ is the relative angular momentum of two nucleons,

$$\vec{L} = \frac{1}{2\hbar}(\vec{r_i} - \vec{r_j}) \times (\vec{p_i} - \vec{p_j}), \tag{2.9}$$

and $\vec{S}$ is the total spin of two nucleons,

$$\vec{S} = \frac{1}{2}(\vec{\sigma}_i + \vec{\sigma}_j). \tag{2.10}$$

The next six operators in Argonne v18 could give a better description on fitting P-wave and D-wave NN scattering data[43]. But the effect is relatively small.

$$O_{ij}^{p=9,14} = [L_{ij}^2, L_{ij}^2(\vec{\sigma}_i \cdot \vec{\sigma}_j), (\vec{L} \cdot \vec{S})^2] \otimes [1, \vec{\tau}_i \cdot \vec{\tau}_j]. \tag{2.11}$$

The last four operators break charge independence, and are written as:

$$O_{ij}^{p=15,18} = T_{ij}, (\vec{\sigma}_i \cdot \vec{\sigma}_j)T_{ij}, S_{ij}T_ij, \tau_i^z + \tau_j^z. \tag{2.12}$$

where T_{ij} is the isotensor,

$$T_{ij} = 3\tau_i^z\tau_j^z - \vec{\tau}_i \cdot \vec{\tau}_j. \tag{2.13}$$

The above 18 operators are the full Argonne v18(AV18) potential. There are other truncated formats of Argonne potentials, written as Argonne vn'[37]. Here 'n' refers the number of the operators in the potential, n is smaller than 18. The prime symbol means that the n operators are not simply truncated from AV18, but are formed from re-generated fitting data, and so their coefficients are not the same as the one in AV18. Typical calculations are done with a simplified potential, preferably v8' or v6', and the remaining contributions calculated perturbatively.

In previous auxiliary field diffusion Monte Carlo, people have used Argonne v6' to calculate the equation state of nuclear matter and light nuclei [26][56][57]. They dropped the spin-orbit operator $\vec{L} \cdot \vec{S}$ and spin-orbit-isospin operator $\vec{L} \cdot \vec{S}(\vec{\tau}_i \cdot \vec{\tau}_j)$. These two operators make the wave function very difficult to diffuse with our basis. In chapter 3, we will explain why the spin-orbit interactions are difficult in Monte Carlo simulations.

In this work, we will add the spin-orbit operator $\vec{L} \cdot \vec{S}$ and spin-orbit-isospin operator $\vec{L} \cdot \vec{S}(\vec{\tau}_i \cdot \vec{\tau}_j)$ to our Hamiltonian. In chapter 4, we will introduce a new

method to propagate these two operators. The potential we are using is Argonne v8'. It has the same format as in equation 2.7, but different $v_p(r_{ij})$ from those in equation 2.6. The following figure is the plot of $v_p(r_{ij})$ versus the two-nucleon distance r_{ij}. In this figure, we can see that at short range, the spin-orbit interactions has much larger coefficient than other non-central potentials. The spin-orbit interaction is expected to change the nuclear matter result by 5 to 10 percent and its perturbative evaluation can not be done at first order, and while the spin-orbit operator includes an additional factor of r_{ij} from the $\vec{L} = \vec{r}_{ij} \times \vec{p}_{ij}$ operator, it is still important to include this part in the two-body potential.

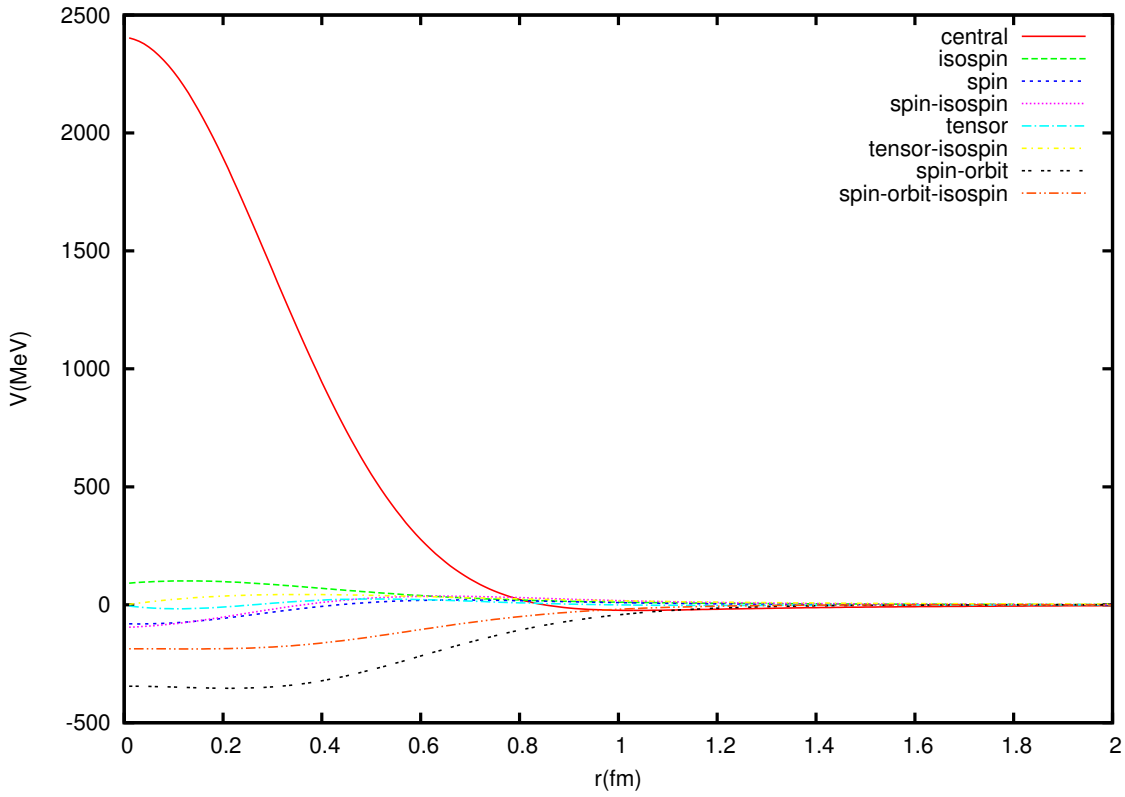

Figure 2.1: 8 Components of AV8'.

2.2 Urbana and Illinois Three-Body Potential

The three-nucleon interactions(TNI) potentials are obtained from two-pion and three-pion exchange and a phenomenological short-range repulsion is fit to the triton and other light nuclei using Green's function Monte Carlo[58][59][60]. They have to be employed with the two-body potentials. The combination of Argonne v18 and Illinois three-body potential(AV18/IL2)[61] has been applied in Green's function Monte Carlo and gives very good results in light nuclei[62][63][64][65][66][67]. Another useful three-body potential is the Urbana potential[68], which shares the same form as the Illinois potential.

$$V_{ijk} = A_{2\pi}^{PW} O_{ijk}^{2\pi,PW} + A_{2\pi}^{SW} O_{ijk}^{2\pi,SW} + A_{3\pi}^{\triangle R} O_{ijk}^{3\pi,\triangle R} + A_R O_{ijk}^R \tag{2.14}$$

The Urbana three-body potential only contains the first and last terms, while the Illinois three-body potential contains all four terms. The A factors are parameters, and the O are three-body spin-isospin operators. The first two terms are the operators for two-pion exchange in the P-wave and S-wave. The third term is three-pion exchange and the last one is a phenomenological short range repulsion. Three nucleons potentials must be applied to get accurate equation of state and nuclear structure, but their inclusion must currently be done using an approximate three-body interaction and the difference with the full three-body interaction calculated perturbatively. Since this does not affect the inclusion of spin-orbit interactions, and the inclusion of any three-body interaction will slow the computations, we do not include them in this work.

Chapter 3

AUXILIARY FIELD DIFFUSION MONTE CARLO

Based on the nucleon-nucleon scattering data and light nuclei spectra, the structure of nuclei has been studied by ab inito methods, such as effective field theory[69][70], no-core shell model, coupled-cluster and Green's function Monte carlo[71]. Though these methods often choose different Hamiltonians and basis sets, the giant integrals and sums of the many-body Schrödinger equation[72] make it difficult to apply them to large system with many nucleons. In 1999, Schmidt and Fantoni developed the auxiliary field diffusion Monte Carlo[27] for use with the Argonne potentials. By introducing an auxiliary field, this method could separate the spin-isospin interactions between two nucleons, and make the calculations much more efficient for the many-nucleon systems.

In this chapter, we will describe how to write the Hamiltonian as a propagator using the auxiliary field diffusion Monte Carlo method, and how to propagate the trial wave function to the ground state. In section 3.1, we will show that the general diffusion Monte Carlo method[73][74][75] can be formalized in the same way as auxiliary field diffusion Monte Carlo. In section 3.2, we will describe auxiliary field diffusion Monte Carlo in detail by employing a Hubbard-Stratonovich transformation[76]. We use this transformation to separate the interactions between two nucleons in Argonne v6'. Then we will add importance sampling[77] to the diffusion process. In section 3.3, the form of the trial wave function will be presented. In section 3.4, we will describe how to use the fixed-phase approximation[78][79][80] to control the fermion sign problem. In section 3.5, we will show the results of auxiliary filed diffusion Monte Carlo for Argonne v6' done by S. Fantoni, S. Gandolfi, F. Pederiva and K.E.

Schmidt[30].

3.1 Diffusion Monte Carlo

We start by describing diffusion Monte Carlo with a central potential. A general diffusion process is employed in both diffusion Monte Carlo and auxiliary field diffusion Monte Carlo. After describing the diffusion process for a central potential, we will discuss how to use the auxiliary field diffusion Monte Carlo to deal with the spin-isospin dependence of our specific Hamiltonian with Argonne v6'.

In diffusion Monte Carlo, we start from Schrödinger equation in imaginary time $\tau = it$, and a trial wave function Ψ_T.

$$-\frac{\partial}{\partial\tau}|\Psi(\tau)\rangle = \hat{H}|\Psi(\tau)\rangle, \tag{3.1}$$

$$|\Psi(0)\rangle = |\Psi_T\rangle. \tag{3.2}$$

The trial wave function Ψ_T should not be orthogonal to the ground-state wave function Ψ_0. Writing it as a linear combination of eigenstates ψ_i of the Hamiltonian.

$$|\Psi_T\rangle = \sum_i c_i|\psi_i\rangle, \tag{3.3}$$

where

$$\hat{H}|\psi_i\rangle = \epsilon_i|\psi_i\rangle. \tag{3.4}$$

From the Schrödinger equation, we have

$$|\Psi(\tau)\rangle = e^{-(\hat{H}-E_T)\tau}|\Psi_T\rangle. \tag{3.5}$$

When $\tau \to \infty$, only the smallest eigenvalue ϵ_0 survives, and $|\Psi(\tau \to \infty)\rangle$ converges to the ground-state wave function. Here we use a trial energy E_T to keep $\langle\Psi_T|\Psi_T(\tau \to \infty)\rangle$ constant.

In the diffusion process, we usually propagate by a small time Δt in each step. After each Δt, the wave function has been propagated to a new distribution, which is closer to the ground-state wave function. After many steps of Δt, the wave function $|\Psi(\tau \to \infty\rangle)$ converges to the ground-state wave function. Therefore, we estimate the ground-state energy as:

$$\langle H\rangle = \frac{\langle \Psi_T|H|\Psi(\tau\to\infty)\rangle}{\langle \Psi_T|\Psi(\tau\to\infty)\rangle}. \tag{3.6}$$

Up to now we have not chosen any particular Hamiltonian. Now let us use this method to solve for the ground state of a Hamiltonian with kinetic energy and a central potential. The wave function only depends on positions, and the Hamiltonian is

$$H = \sum_{i=1}^{A} \frac{p_i^2}{2m} + v(R), \tag{3.7}$$

and R represents the 3A coordinates of the A particles. From Equation (3.5), after a small time step Δt, we have

$$\langle R|\Psi(t+\Delta t)\rangle = \int \mathrm{d}R' \langle R|e^{-(\sum_i \frac{p_i^2}{2m} + v(R) - E_T)\Delta t}|R'\rangle\langle R'|\Psi(t)\rangle. \tag{3.8}$$

For small Δt, we can approximate the exponential by $e^{-\frac{(v(R)-E_T)\Delta t}{2}} e^{-\sum_i \frac{p_i^2\Delta t}{2m}} e^{-\frac{(v(R')-E_T)\Delta t}{2}}$. For the kinetic energy part, by using a Fourier transform, we have:

$$\langle R|e^{-\sum_i \frac{p_i^2\Delta t}{2m}}|R'\rangle = \int \frac{d^{3A}k}{(2\pi)^{3A}} e^{i\vec{k}\cdot\vec{R}} e^{-\frac{\hbar^2 k^2 \Delta t}{2m}} e^{-i\vec{k}\cdot\vec{R}'}, \tag{3.9}$$

which gives the free-particle Green's function

$$\langle R|e^{-\sum_i \frac{p_i^2\Delta t}{2m}}|R'\rangle = G_0(R,R',\Delta t) = (\frac{m}{2\pi\hbar^2\Delta t})^{\frac{3A}{2}} e^{-\frac{m(R-R')^2}{2\hbar^2\Delta t}}. \tag{3.10}$$

Then we have the wave propagation function as

$$\Psi(R,\Delta t) = \int \mathrm{d}R' G(R,R',\Delta t)\Psi_T(R'), \tag{3.11}$$

where the whole Green's function is

$$G(R, R', \Delta t) = e^{-\frac{(v(R)-E_T)\Delta t}{2}} G_0(R, R', \Delta t) e^{-\frac{(v(R')-E_T)\Delta t}{2}}. \tag{3.12}$$

In diffusion Monte Carlo, the kinetic energy part is non-local and the Gaussian changes the wave function to a new distribution as in diffusion, so it is called the diffusion part. The potential is local and be interpreted as a weight for the Monte Carlo sampling of the new distribution, so it is often called the branching part.

3.2 Auxiliary Field Diffusion Monte Carlo

In the central potential example in section 3.1, the wave function $\langle R|\Psi(t)\rangle$ only depends on position. Each nucleon could be diffused independently, with different weights. In diffusion Monte Carlo, we usually use the term 'walker' to indicate a sample of these nucleons. Each walker consists of the 3A position coordinates of the A particle. Those walkers are propagated by $e^{-(\hat{H}-E_T)t}$ from any initial distribution to the ground state of the Hamiltonian. After each step of propagation, a walker diffuses to a new position and gets a new weight. This weight is sampled to give zero, one, or more new walkers.

In nuclear matter, there are spin and isospin interactions between the nucleons. These interactions make the possible number of spin-isospin states increase exponentially with the increase of the number of nucleons. All of their possible states are kept with coefficients in Green's function Monte Carlo, which makes it difficult to apply Green's function Monte Carlo to more than A=12. To solve this problem, auxiliary field diffusion Monte Carlo introduces a single spinor to describe each nucleon and then the computational scaling is reduced from exponential to polynomial. This

makes it possible to calculate heavier nuclei.

3.2.1 General Form

From section 3.1, we know that the general diffusion of state with time step Δt is:

$$|\Psi(t+\Delta t)\rangle = e^{-(\hat{H}-E_T)\Delta t}|\Psi(t)\rangle, \tag{3.13}$$

where $e^{-(\hat{H}-E_T)\Delta t}$ is the propagator. In the central potential example, the propagator could be written as:

$$\langle R|e^{-(\hat{H}-E_T)\Delta t}|R'\rangle = G(R,R',\Delta t). \tag{3.14}$$

The Green's function in equation 3.14 is a Gaussian distribution, multiplied by the exponential of the potential times time step. The right hand side of equation 3.14 could be interpreted as a propagator sampled from Gaussian distribution. So equation 3.14 could be written in a more general form:

$$e^{-(\hat{H}-E_T)\Delta t} = \int \mathrm{d}X P(X) T(X), \tag{3.15}$$

where P(X) is a Gaussian distribution, T(X) is a walker translation operator. Though P(X) could be other distributions for other propagator forms, it is a Gaussian distribution in this work.

In the Argonne two-body potential, there are a central potential and potentials with spin/isospin operators. The central force only depends on positions, and the spin/isospin operators will rotate the spinor of each nucleon. So we use the basis $|RS\rangle$ for each walker. 'R' stands for 3-dimension positions. 'S' stands for 4 spinors, which are given by the amplitude to be in $p\uparrow$, $p\downarrow$, $n\uparrow$ and $n\downarrow$. Then the state is a

linear combination of the walkers.

$$|\Psi(t)\rangle = \sum_i w_i |R_i S_i\rangle, \tag{3.16}$$

where i is a label for the walker state, w_i is the weight for each walker. After one time step, the new state is:

$$|\Psi(t+\Delta t)\rangle = \sum_i w_i \int \mathrm{d}X P(X) T(X) |R_i S_i\rangle \tag{3.17}$$

However, this integral is not efficiently sampled, since the result will have large variance. To reduce the variance, we add importance sampling $|\Psi_I\rangle$. Then the left-hand side of equation 3.17 becomes $|\Psi_I \Psi(t+\Delta t)\rangle$, where

$$\langle RS|\Psi_I \Psi(t)\rangle = \langle \Psi_I|RS\rangle \langle RS|\Psi(t)\rangle \tag{3.18}$$

The right-hand side of equation 3.17 needs to be multiplied by the ratio $\frac{\langle \Psi_I|R'S'\rangle}{\langle \Psi_I|RS\rangle}$, where the $|R'S'\rangle$ is the new state after one time step propagation. The $\langle \Psi_I|RS\rangle$ in the denominator divides out importance function in $|\Psi_I \Psi(t)\rangle$ and the $\langle \Psi_I|R'S'\rangle$ in the numerator then produces the similar term for $|\Psi_I \Psi(t+\Delta t)\rangle$ So the propagation with importance sampling becomes:

$$|\Psi_I \Psi(t+\Delta t)\rangle = \sum_i w_i \int \mathrm{d}X \frac{\langle \Psi_I|R'_i S'_i\rangle}{\langle \Psi_I|R_i S_i\rangle} P(X) T(X) |R_i S_i\rangle. \tag{3.19}$$

The equation 3.19 propagates the walkers for small time step with importance sampling. Our walkers $|R_i S_i\rangle$ are diffused to the new state $|R'_i S'_i\rangle$ by the operator T(X). X are sampled from the normalized distribution $P(X)\frac{\langle \Psi_I|T(X)|R_i S_i\rangle}{\langle \Psi_I|R_i S_i\rangle}$. The weight of the propagation for each walker is $w_i \frac{\langle \Psi_I|R'S'\rangle}{\langle \Psi_I|RS\rangle}$. The normalization is calculated as

$$\begin{aligned} N &= \int \mathrm{d}X P(X) \frac{\langle \Psi_I|T(X)|R_i S_i\rangle}{\langle \Psi_I|R_i S_i\rangle} \\ &= \frac{\langle \Psi_I|e^{-(\hat{H}-E_T)\Delta t}|R_i S_i\rangle}{\langle \Psi_I|R_i S_i\rangle} \\ &= e^{-(E_L(R_i,S_i)-E_T)\Delta t}. \end{aligned} \tag{3.20}$$

The local energy $E_L(R_i, S_i)$ is calculated as:

$$E_L(R_i, S_i) = \frac{\langle \Psi_I | H | R_i S_i \rangle}{\langle \Psi_I | R_i S_i \rangle}. \tag{3.21}$$

So after every small time step propagation, we need to sample the normalized X distribution and include the normalization in the weight.

3.2.2 Application to Argonne v6'

The Argonne v6' potential consists of 6 operators. The Hamiltonian is

$$H = \sum_{i=1}^{A} \frac{p_i^2}{2m} + \sum_{i<j} \sum_{p=1}^{6} v_p(r_{ij}) O_{ij}^p, \tag{3.22}$$

with the 6 operators

$$1, \vec{\tau}_i \cdot \vec{\tau}_j, \vec{\sigma}_i \cdot \vec{\sigma}_j, (\vec{\sigma}_i \cdot \vec{\sigma}_j)(\vec{\tau}_i \cdot \vec{\tau}_j), S_{ij}, S_{ij}(\vec{\tau}_i \cdot \vec{\tau}_j), \tag{3.23}$$

where the first one is central force, S_{ij} is tensor, $S_{ij} = 3\vec{\sigma}_i \cdot \hat{r}_{ij} \vec{\sigma}_j \cdot \hat{r}_{ij} - \vec{\sigma}_i \cdot \vec{\sigma}_j$. The equation 3.19 could not be directly applied to operators like $\vec{\sigma}_i \cdot \vec{\sigma}_j$. Because in equation 3.19, the T(X) must change one walker $|R_i S_i\rangle$ into a single new one $|R_i' S_i'\rangle$. The operator $\vec{\sigma}_i \cdot \vec{\sigma}_j$ will change $|R_i S_i\rangle$ into a linear combination of new $|R_i' S_i'\rangle$. To write the propagator in the form of equation 3.19, the auxiliary field diffusion Monte Carlo method employs a Hubbard-Stratonovich transformation to break up the interactions, so that the propagator is linear in the particle spinors and give a single walker from a single sample of X. The main idea is that, we write the potentials in quadratic forms first, and then use Hubbard-Stratonovich transformation to linearise the operators with exponentials in the propagator.

Take $\vec{\sigma}_i \cdot \vec{\sigma}_j$ for example. Write it in the three components of Pauli operators,

$$\sum_{ij} v^{\sigma}(r_{ij}) \vec{\sigma}_i \cdot \vec{\sigma}_j = \frac{1}{2} \sum_{ij}^{A} \sigma_{ix} B_{ij} \sigma_{jx} + \frac{1}{2} \sum_{ij}^{A} \sigma_{iy} B_{ij} \sigma_{jy} + \frac{1}{2} \sum_{ij}^{A} \sigma_{iz} B_{ij} \sigma_{jz}, \tag{3.24}$$

where $B_{ii} = 0$, $B_{ij} = v^{\sigma}(r_{ij})$ for $i \neq j$, B_{ij} is real and symmetric. The eigenvectors and eigenvalues of B_{ij} can be calculated by numerically diagonalizing the matrix B_{ij}. We write

$$\begin{aligned} \sum_j B_{ij}\psi_j^{(n)} &= \lambda_n \psi_i^{(n)}, \\ \sum_j \psi_j^{(n)}\psi_j^{(m)} &= \delta_{nm}. \end{aligned} \tag{3.25}$$

The B_{ij} matrix is then

$$B_{ij} = \sum_n \psi_i^{(n)} \lambda_n \psi_j^{(n)}. \tag{3.26}$$

The the first term in equation 3.24 becomes:

$$\frac{1}{2}\sum_{ij}^{A} \sigma_{ix} B_{ij} \sigma_{jx} = \frac{1}{2}\sum_n \lambda_n (O_{nx})^2, \tag{3.27}$$

$$O_{nx} = \sum_{i=1}^{A} \psi_i^{(n)} \sigma_{ix}. \tag{3.28}$$

Therefore, the spin operator term could be written as a sum of squares of operators.

$$\sum_{ij} v^{\sigma}(r_{ij}) \vec{\sigma}_i \cdot \vec{\sigma}_j = \frac{1}{2}\sum_n \lambda_n (O_{nx})^2 + \frac{1}{2}\sum_n \lambda_n (O_{ny})^2 + \frac{1}{2}\sum_n \lambda_n (O_{nz})^2, \tag{3.29}$$

where

$$\begin{aligned} O_{nx} &= \sum_{i=1}^{A} \psi_i^{(n)} \sigma_{ix}, \\ O_{ny} &= \sum_{i=1}^{A} \psi_i^{(n)} \sigma_{iy}, \\ O_{nz} &= \sum_{i=1}^{A} \psi_i^{(n)} \sigma_{iz}. \end{aligned} \tag{3.30}$$

In order to write the whole Hamiltonian in quadratic forms, we re-organize the spin-isospin potentials in three parts: spin part, including spin and tensor operators;

isospin operator; and spin-isospin part, including spin-isospin operators and tensor-isospin operators.

$$\begin{aligned} H =& \sum_{i\alpha} \frac{p_{i\alpha}^2}{2m} + \sum_{i<j} v^c(r_{ij}) + \sum_{i<j,\gamma} v^\tau(r_{ij})\tau_{i\gamma}\tau_{j\gamma} \\ &+ \sum_{i<j,\alpha\beta} \{v^\sigma r(r_{ij}\delta_{\alpha\beta}) + v^t(r_{ij})[3\hat{\alpha}\cdot\hat{r}_{ij}\hat{\beta}\cdot\hat{r}_{ij} - \delta_{\alpha\beta}]\}\sigma_{i\alpha}\sigma_{j\beta} \\ &+ \sum_{i<j,\alpha\beta\gamma} \{v^{\sigma\tau}(r_{ij})\delta_{\sigma\beta} + v^{t\tau}(r_{ij})[3\hat{\alpha}\cdot\hat{r}_{ij}\hat{\beta}\cdot\hat{r}_{ij} - \delta_{\alpha\beta}]\}[\sigma_{i\alpha}\tau_{i\gamma}][\sigma_{j\beta}\tau_{j\gamma}]. \end{aligned} \tag{3.31}$$

α, β, γ are summed over the x, y, z components. The superscripts c, τ, σ, t are notations for the central force, isospin, spin, and tensor parts. $\hat{\alpha}, \hat{\beta}$ are unit vectors. For the last three terms in equation 3.31, we could use the technique described above for $\vec{\sigma}_i \cdot \vec{\sigma}_j$ to rewrite them in quadratic forms. First, we determine the matrices which correspond to nucleon i and j interacting,

$$\begin{aligned} C_{ij}^\tau &= v^\tau(r_{ij}), \\ C_{i\alpha,j\beta}^\sigma &= v^\sigma(r_{ij})\delta_{\alpha\beta} + v^t(r_{ij})[3\hat{\alpha}\cdot\hat{r}_{ij}\hat{\beta}\cdot\hat{r}_{ij} - \delta_{\alpha\beta}], \\ C_{i\alpha,j\beta}^{\sigma\tau} &= v^{\sigma\tau}(r_{ij})\delta_{\alpha\beta} + v^{t\tau}(r_{ij})[3\hat{\alpha}\cdot\hat{r}_{ij}\hat{\beta}\cdot\hat{r}_{ij} - \delta_{\alpha\beta}]. \end{aligned} \tag{3.32}$$

Then we calculate the eigenvectors and eigenvalues for the C_{ij} matrices.

$$\begin{aligned} \sum_j C_{ij}^\tau \psi_j^{\tau(n)} &= \lambda_n^\tau \psi_i^{\tau(n)}, \\ \sum_{j\beta} C_{i\alpha,j\beta}^\sigma \psi_{j\beta}^{\sigma(n)} &= \lambda_n^\sigma \psi_{i\alpha}^{\sigma(n)}, \\ \sum_{j\beta} C_{i\alpha,j\beta}^{\sigma\tau} \psi_{j\beta}^{\sigma(n)} &= \lambda_n^{\sigma\tau} \psi_{i\alpha}^{\sigma\tau(n)}. \end{aligned} \tag{3.33}$$

Therefore, the Hamiltonian could be written as,

$$\begin{aligned} H =& \sum_{i\alpha} \frac{p_{i\alpha}^2}{2m} + \sum_{i<j} v^c(r_{ij}) + \frac{1}{2}\sum_{n=1}^{A}\sum_{\alpha=1}^{3} \lambda_n^\tau (O_{n\alpha}^\tau)^2 \\ &+ \frac{1}{2}\sum_{n=1}^{3A} \lambda_n^\sigma (O_n^\sigma)^2 + \frac{1}{2}\sum_{n=1}^{3A}\sum_{\alpha=1}^{3} \lambda_n^{\sigma\tau} (O_{n\alpha}^{\sigma\tau})^2, \end{aligned} \tag{3.34}$$

where

$$O^{\tau}_{n\alpha} = \sum_{i} \psi_{i}^{\tau(n)} \tau_{i\alpha},$$
$$O^{\sigma}_{n} = \sum_{i\alpha} \psi_{i\alpha}^{\sigma(n)} \sigma_{i\alpha}, \tag{3.35}$$
$$O^{\sigma\tau}_{n\beta} = \sum_{i\alpha} \psi_{i\alpha}^{\sigma\tau(n)} \sigma_{i\alpha}\tau_{i\beta}.$$

We will now use the Hubbard-Stratonovich transformation to linearise the operators in equation 3.34, so that they can propagate the state as in equation 3.19. The Hubbard-Stratonovich transformation is the operator identity:

$$e^{\frac{O^2}{2}} = \frac{1}{\sqrt{2\pi}} \int_{-\infty}^{\infty} \mathrm{d}x e^{-\frac{x^2}{2}} e^{xO} \tag{3.36}$$

The x in equation 3.36 is called the auxiliary field. By introducing this field, the operator O^2 are linearised. The distribution of the auxiliary field is a Gaussian distribution since the left-hand side has the operators squared in the exponent. After using importance sampling, the distribution of x will correspond to a shifted Gaussian, which we will explain later.

Then the quadratic operators in equation 3.34 could be used in equation 3.36. Take $\frac{1}{2}\sum \lambda_n^{\sigma}(O_n^{\sigma})^2$ for example.

$$e^{-\frac{1}{2}\sum_{n=1}^{3A} \lambda_n^{\sigma}(O_n^{\sigma})^2 \Delta t} = \int \mathrm{d}x \frac{1}{(2\pi)^{3A/2}} e^{-\frac{1}{2}\sum_{n=1}^{3A} x_n^2} e^{-i\sum_{n=1}^{3A} x_n \sqrt{\lambda_n \Delta t} O_n^{\sigma}}. \tag{3.37}$$

Equation 3.37 has the same form as equation 3.17. By using auxiliary field x_n, the quadratic operators $\frac{1}{2}\sum \lambda_n^{\sigma}(O_n^{\sigma})^2$ could be linearised. So can the other spin-isospin operators in equation 3.34. Therefore, our walkers can now be propagated from one walker state to a single new one. That is, after sampling the x_n values, the right hand side of equation 3.37 rotates and scales the spinors for each particle in the walkers.

We also could include importance sampling in Hubbard-Stratonovich transformation. We keep taking $\frac{1}{2}\sum \lambda_n^{\sigma}(O_n^{\sigma})^2$ as example. From section 3.2.1, we know that

adding importance sampling is equivalent to including the ratio of new importance functions in the propagation. Also, the sampling needs to be normalized. If we normalize the importance sampling with the whole Hamiltonian like in equation 3.20, the normalization gives an extral weight $e^{-(E_L(R_i,S_i)-E_T)\Delta t}$. Then, to include the importance sampling in the auxiliary field, we could expand the propagator in equation 3.37 with the normalized sampling, and truncate the expansion to order Δt^2. We find that the sampling becomes a shifted Gaussian:

$$x_n = \chi_n - i\sqrt{\lambda_n \Delta t}\langle O_n^\sigma \rangle, \tag{3.38}$$

where the χ_n is a Gaussian distribution. This is how the Argonne v6' potential has been applied to auxiliary field diffusion Monte Carlo. Let us sum up the whole process: first, we rewrite the Hamiltonian as a sum of squared operators. Then we introduce an auxiliary field with the Hubbard-Stratonovich transformation to linearize the operators in the exponential of the propagator; with this form, the propagation scales with polynomial order in the particle number. By adding importance sampling, the auxiliary field became a shifted Gaussian. Finally, our wave function could be propagated by the linearised operators with the shifted Gaussian. And the weight of the new walker is the normalization factor.

3.3 Trial Wave Function

The trial wave function that we are using for nuclear matter is the product of the Jastrow function and a Slater determinant.

$$\Psi_T(R,S) = \Phi_S(R)\Phi_A(R,S) \tag{3.39}$$

$\Phi_S(R)$ is the symmetric Jastrow function depending on the distance between nu-

cleons. It has a form as

$$\Phi_S(R) = \prod_{i<j} f_J(r_{ij}). \tag{3.40}$$

The function $f_J(r_{ij})$ is the central function calculated in the single-operator chain approximation of the Fermi Hypernetted Chain(FHNC/SOC). The Jastrow function only reduces the variance of the ground-state energy, without changing the phase of the wave function.

$\Phi_A(R, S)$ is the antisymmetric Slater determinant of single nucleon. For nuclear matter, we use free-particle orbitals in a periodic box with side L. So the wave vectors are:

$$\vec{k} = \frac{2\pi}{L}(n_x, n_y, n_z). \tag{3.41}$$

The spatial part of the single-particle orbital are plane waves $e^{i\vec{k}\cdot\vec{r}}$. The spinor part is expressed in a basis of proton-up, proton-down, neutron-up, neutron-down, written as $|p\uparrow, p\downarrow, n\uparrow, n\downarrow\rangle$. So the element in the Slater determinant is:

$$\phi_{ij} = \langle \vec{r}_i \vec{s}_i | \phi_j \rangle, \tag{3.42}$$

and the $\langle \vec{r}_i \vec{s}_i | \phi_j \rangle$ are one of the four orbitals

$$\langle \vec{r}_i, \vec{s}_i | \phi_j \rangle = e^{i\vec{k}_j\cdot\vec{r}_i}\delta_{s_i,p\uparrow},\ e^{i\vec{k}_j\cdot\vec{r}_i}\delta_{s_i,p\downarrow},\ e^{i\vec{k}_j\cdot\vec{r}_i}\delta_{s_i,n\uparrow},\ or\ e^{i\vec{k}_j\cdot\vec{r}_i}\delta_{s_i,n\downarrow}. \tag{3.43}$$

This is the trial wave function that we are using in auxiliary field diffusion Monte Carlo. We also use this trial wave function as the importance function. By sampling the shifted Gaussian x_n, the Hamiltonian with Argonne v6' could propagate the positions and spinors of walkers separately to a new state, and we then calculate the mixed-energy expected value of Hamiltonian with that state as in equation 3.6.

3.4 Fixed-Phase Approximation

The simulations of fermions always encounter the Fermi sign problem. The fixed-phase approximation was developed to constrain the wave function of electrons in magnetic field, to get an upper bound to the ground-state energy.

In nuclear matter, the wave function is complex. The fixed-phase approximation is developed to constrain the phase of the propagated wave function to be the same as the phase of the trial wave function. That is, after propagation we take the real part of the weight. The fixed-phase approximation is usually used in Fermi system.

3.5 Result of Argonne v6' in AFDMC

Based on the Hamiltonian introduced in chapter 2, and auxiliary field diffusion Monte Carlo described in chapter 3, the ground-state energy of nuclear matter at low energy could be calculated and the equation of state(EOS)[81] could be obtained. The EOS in nuclear matter[82][83] can be applied to nuclei[84][85], neutron stars[2], heavy-ion collision[7][86], and astronuclear physics[87][88]. In this section, we will show the result of Argonne v6' in nuclear matter.

We calculate the ground-state energy for 28 nucleons, which is the first closed shell. There are 14 protons and 14 neutrons. The density is from $0.08fm^{-3}$ to $0.48fm^{-3}$. The results of ground-state energy at each density are listed with error bars in table 3.1.

From the results, we can see that there is a minimum energy in nuclear matter as a function of density. But this equilibrium point is not at saturation density $\rho_0 = 0.16(fm^{-3})$ calculated from the semi-empirical mass formula. That is because we

Table 3.1: AFDMC in v6'

$\rho(fm^{-3})$	mean value(MeV)	error bar(MeV)
0.08	-7.31	0.16
0.16	-11.97	0.24
0.24	-15.02	0.32
0.32	-15.62	0.46
0.40	-13.01	1.15
0.48	-10.99	1.14

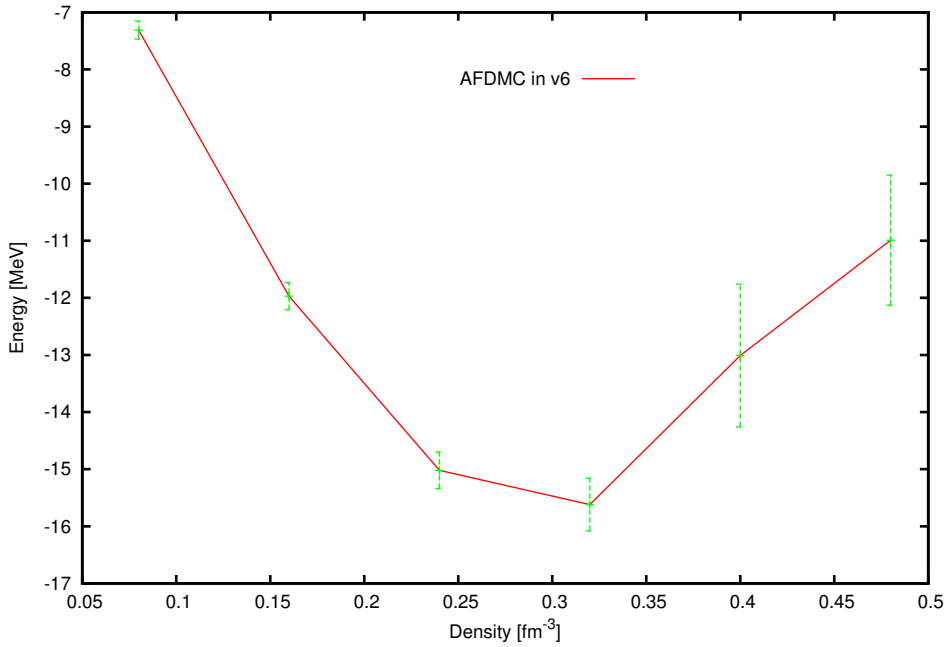

Figure 3.1: AFDMC in v6'

have not included three-body potential. So after solving the spin-orbit interactions, the three-body potential needs to be included too[89]. We plot the ground-state energy against density in figure 3.1. It shows that as the density increases, the variance increases as well.

Chapter 4

SPIN-ORBIT INTERACTIONS

In the last chapter, we showed how previous work used the auxiliary field diffusion Monte Carlo method to obtain equation of state of nuclear matter with the Hamiltonian for Argonne v6'. However, those results did not include the spin-orbit interactions. Because in nuclear matter, there are isospin-dependent spin-orbit interactions, which are different in isosinglet and isotriplet states. The isospin operators will rotate the isospin of the two nucleons subject to the spin-orbit interactions, and make the integral scaling increase exponentially with the number of nucleons, unless a linearization can be performed in the propagation exponent. That is the difficult part to calculate spin-orbit interactions in nuclear matter, because there are effectively three operators, momentum along with 2 spin/isospin operators, so that it can not be written as sum of squares as before. In this chapter, we will use a second auxiliary field to linearize the interactions between nucleons, so that we can calculate the spin-orbit interactions in nuclear matter.

Before we introduce the spin-orbit interactions in nuclear matter, we would like to introduce the spin-orbit interactions in neutron matter as done by other researchers [90][91]. The spin-orbit interaction in neutron matter is easier to calculate than in nuclear matter. This is because it can be written as squares of operators. Pairs of neutrons are always in triplets in neutron matter, and their form does not bring exponential scaling to method, so the spin-orbit interactions could be simulated with the same complexity as Argonne v6'. But this work is meaningful because we can see how the spin-orbit interaction can change the ground-state energy in neutron matter.

In section 4.1, we will describe the spin-orbit interactions in neutron matter as

done in reference[91]. Then we will present a new method called pair-wise propagation to calculate the spin-orbit interaction in neutron matter. This new method is a different linearization in contrast to the method previously used. It uses a pair-wise propagation break up. The reason that we developed this pair-wise propagation is that we could extend this new propagation method to the interactions between nucleons in nuclear matter. In section 4.2, we will show how we use this pair-wise propagation with a second auxiliary field to calculate the spin-orbit with isospin interactions in nuclear matter.

4.1 Spin-Orbit Interactions in Neutron Matter

Simulation of neutron matter is important to the study of the equation of state and other properties of neutron stars. Green's function Monte Carlo[92] has been used to calculate small neutron drops bound in external potential wells[94][95] because they are small enough to be calculated and give some idea of the equation of state. Auxiliary field diffusion Monte Carlo gives good agreement with Green's function Monte Carlo with energies within 2% for an 8-neutron drop[96]. However, in both calculations the difference of the energies of different spin states of 7-neutron drops shows that the spin-orbit interactions must be included.

The potential used previously is Argonne v8'. From section 3.2.2, we know that the Hamiltonian needs to be written as the sum of squares for the auxiliary field method to be applied. So the main idea to solve the spin-orbit interaction is to combine these spin/isospin parts with the momentum operator, and write the various parts as sum of squares of operators. Based on this idea, we developed the pair-wise propagation for the spin-orbit interactions and kinetic energy.

The Hamiltonian with Argonne v8' has the same form as equation 3.20, but the coefficients $v_p(r_{ij})$ are different, since the potential is refit and truncated.

$$H = \sum_{i=1}^{A} \frac{p_i^2}{2m} + \sum_{i<j} \sum_{p=1}^{8} v_p(r_{ij}) O_{ij}^p, \tag{4.1}$$

where the 8 operators O_{ij}^p are:

$$1, \vec{\tau}_i \cdot \vec{\tau}_j, \vec{\sigma}_i \cdot \vec{\sigma}_j, (\vec{\sigma}_i \cdot \vec{\sigma}_j)(\vec{\tau}_i \cdot \vec{\tau}_j), S_{ij}, S_{ij}(\vec{\tau}_i \cdot \vec{\tau}_j), \vec{L} \cdot \vec{S}, \vec{L} \cdot \vec{S}(\vec{\tau}_i \cdot \vec{\tau}_j). \tag{4.2}$$

The first 6 operators in equation 4.2 have already been written as sum of squares as in equation 3.34, except central force, which is trivially included. Now we need to write the two spin-orbit terms $\vec{L} \cdot \vec{S}$ and $\vec{L} \cdot \vec{S}(\vec{\tau}_i \cdot \vec{\tau}_j)$ as sums of squares too. These two operators have a momentum part, so we combine these two operators with the kinetic energy part and call this part of Hamiltonian H_r, written as follows.

$$H_r = \sum_i \frac{p_i^2}{2m} + \sum_{i<j} v_{ls}(r_{ij}) \vec{L}_{ij} \cdot \vec{S}_{ij} + \sum_{i<j} v_{ls\tau}(r_{ij}) \vec{L}_{ij} \cdot \vec{S}_{ij} (\vec{\tau}_i \cdot \vec{\tau}_j). \tag{4.3}$$

The kinetic energy can be separated into the center-of-mass and relative pieces.

$$\sum_i \frac{p_i^2}{2m} = \frac{P^2}{2mA} + \sum_{i<j} \frac{p_{ij}^2}{\frac{1}{2}mA}. \tag{4.4}$$

The center of mass piece $\frac{P^2}{2mA}$ can be dropped in our case, since our wave functions are eigenvalues of $\vec{P}$ with eigenvalue zero. Also, for the other two terms in equation 4.3, we have:

$$\vec{L}_{ij} = \frac{1}{\hbar}(\vec{r}_i - \vec{r}_j) \times \vec{p}_{ij}, \tag{4.5}$$

where we define the angular momentum to be unitless and

$$\vec{p}_{ij} = \frac{1}{2}(\vec{p}_i - \vec{p}_j), \tag{4.6}$$

and $\vec{S}_{ij}$ is the total spin of two nucleons.

$$\vec{S}_{ij} = \frac{1}{2}(\vec{\sigma}_i + \vec{\sigma}_j). \tag{4.7}$$

The Hamiltonian H_r becomes:

$$\begin{aligned} H_r &= \sum_{i<j} \frac{p_{ij}^2}{\frac{1}{2}mA} + \sum_{i<j} \frac{1}{2\hbar}\{[(\vec{r}_i - \vec{r}_j) \times \vec{p}_{ij}] \cdot (\vec{\sigma}_i + \vec{\sigma}_j)\}[v_{ls}(r_{ij}) + \vec{\tau}_i \cdot \vec{\tau}_j v_{ls\tau}(r_{ij})] \\ &= \sum_{i<j} \left\{ \frac{p_{ij}^2}{\frac{1}{2}mA} + \vec{p}_{ij} \cdot \frac{1}{2\hbar}[(\vec{\sigma}_i + \vec{\sigma}_j) \times \vec{r}_{ij}][v_{ls}(r_{ij}) + \vec{\tau}_i \cdot \vec{\tau}_j v_{ls\tau}(r_{ij})] \right\}. \end{aligned} \tag{4.8}$$

The $\vec{\tau}_i \cdot \vec{\tau}_j$ is one in neutron matter, so we can combine the v_{ls} and $v_{ls\tau}$ as a single potential:

$$v'_{ls}(r_{ij}) = v_{ls}(r_{ij}) + v_{ls\tau}(r_{ij}), \tag{4.9}$$

and write the equation 4.8 in a quadratic form as the following:

$$\begin{aligned} H_r = &\sum_{i<j} \frac{2}{mA} \left(\vec{p}_{ij} + \frac{mA}{8\hbar}[(\vec{\sigma}_i + \vec{\sigma}_j) \times \vec{r}_{ij}] v'_{ls}(r_{ij}) \right)^2 \\ &- \sum_{i<j} \frac{mA}{32\hbar^2}[(\vec{\sigma}_i + \vec{\sigma}_j) \times \vec{r}_{ij}]^2 (v'_{ls}(r_{ij}))^2. \end{aligned} \tag{4.10}$$

We have written all the operators for neutron matter in equation 4.1 as the sum of squares. Now we can use a Hubbard-Stratonovich transformation to linearise these operators in the propagator exponent. The first six operators in equation 4.2 are linearised as before. So we only need to deal with the new H_r.

For the right-hand side of equation 4.10, the second term is called a counter term. It is a local potential and has the same form as the first six operators in equation 4.2. So we combine them together and operate on the wave functions exactly as we did with Argonne v6' for these terms. We write:

$$v_{counter} = -\sum_{i<j} \frac{mA}{32\hbar^2}[(\vec{\sigma}_i + \vec{\sigma}_j) \times \vec{r}_{ij}]^2 (v'_{ls}(r_{ij}))^2. \tag{4.11}$$

For the first term on the right-hand side of equation 4.10, after application of the Hubbard-Stratonovich transformation, the momentum part and spin part will act separately in the exponent, so that the position basis $|R\rangle$ and spin basis $|S\rangle$ propagate independently. In the pair-wise propagation, instead of a Hubbard-Stratonovich

breakup for the full Hamiltonian, we break up the pair-wise parts separately. That is, the positions of a pair of nucleons will be translated by the momentum operator $\vec{p}_{ij}$ simultaneously. And the spinors of that pair will be rotated by the spin operator $\vec{S}_{ij}$ in a correlated way.

We first write H_r as a propagator in the form of equation 3.37:

$$\begin{aligned} e^{-H_r\Delta t} = & \prod_{i<j} \frac{1}{(2\pi)^{\frac{3}{2}}} \int \mathrm{d}^3 x_{ij} \mathrm{e}^{-\frac{|\vec{x}_{ij}|^2}{2}} \mathrm{e}^{-\frac{i}{\hbar}\sqrt{\frac{4\hbar^2\Delta t}{mA}}\left(\vec{p}_{ij}+\frac{mA}{8\hbar}[(\vec{\sigma}_i+\vec{\sigma}_j)\times\vec{r}_{ij}](v'_{ls}(r_{ij}))\right)\cdot\vec{x}_{ij}} \\ & \cdot \mathrm{e}^{\frac{mA\Delta t}{32\hbar^2}[(\vec{\sigma}_i+\vec{\sigma}_j)\times\vec{r}_{ij}]^2(v'_{ls}(r_{ij}))^2}. \end{aligned} \tag{4.12}$$

The counter terms in the propagator do not depend on the momentum operator. It could be moved out of the integral, and combined with the rest of the potential. The $\vec{x}_{ij}$ is the introduced auxiliary field. From the previous chapter, we know that it can be sampled in with the importance sampling form:

$$\vec{x}_{ij} = \vec{\chi}_{ij} - i\sqrt{\lambda_{ij}\Delta t}\langle\vec{O}_{ij}\rangle. \tag{4.13}$$

$\vec{\chi}_{ij}$ is a Gaussian distribution with unit variance. From equation 4.12, we can see that in our case,

$$\lambda_{ij} = \frac{4}{mA}, \tag{4.14}$$

$$\vec{O}_{ij} = \vec{p}_{ij} + \frac{mA}{8\hbar}[(\vec{\sigma}_i + \vec{\sigma}_j) \times \vec{r}_{ij}]v'_{ls}(r_{ij}). \tag{4.15}$$

Substituting equation 4.14 and 4.15 into equation 4.13, the auxiliary field $\vec{x}_{ij\alpha}$ becomes:

$$\vec{x}_{ij} = \vec{\chi}_{ij} - \sqrt{\frac{4\Delta t}{mA}}\langle\vec{p}_{ij}\rangle - i\sqrt{\frac{mA\Delta t}{16\hbar^2}}\langle(\vec{\sigma}_i + \vec{\sigma}_j) \times \vec{r}_{ij}\rangle v'_{ls}(r_{ij}). \tag{4.16}$$

We will use this shifted Gaussian to propagate our walkers $|RS\rangle$ in the pair-wise method. First, we propagate the momentum operator $\mathrm{e}^{-\frac{i}{\hbar}\sqrt{\frac{4\Delta t\hbar^2}{mA}}\vec{p}_{ij}\cdot\vec{x}_{ij}}$. Since $\mathrm{e}^{-\frac{i}{\hbar}\vec{p}_{ij}\cdot\vec{a}}$ will translate $|\vec{R}_{ij}\rangle$ by $\vec{a}$. We have

$$\vec{R'}_{ij} = \vec{R}_{ij} + \vec{x}_{ij}\sqrt{\frac{4\Delta t\hbar^2}{mA}}. \tag{4.17}$$

Substituting (4.16) in to (4.17), and using the fixed-phase approximation, we have

$$\begin{aligned}\vec{R'}_{ij} =&\vec{R}_{ij} + \vec{\chi}_{ij}\sqrt{\frac{4\Delta t\hbar^2}{mA}} - \frac{4\Delta t\hbar}{mA}\langle\vec{p}_{ij}\rangle \\ &- \mathrm{Re}\left[i\frac{\Delta t}{2}\langle(\vec{\sigma}_i + \vec{\sigma}_j)\times\vec{r}_{ij}\rangle v'_{ls}(r_{ij})\right].\end{aligned} \tag{4.18}$$

Let us use a simpler notation for the new relative coordinate of the pairs.

$$\vec{R}_{diff} = \vec{\chi}_{ij}\sqrt{\frac{4\Delta t\hbar^2}{mA}} - \frac{4\Delta t\hbar}{mA}\langle\vec{p}_{ij}\rangle - \mathrm{Re}\left[i\frac{\Delta t}{2}\langle(\vec{\sigma}_i + \vec{\sigma}_j)\times\vec{r}_{ij}\rangle v'_{ls}(r_{ij})\right]. \tag{4.19}$$

Then for particle i and j in the pair, their positions will be translated as:

$$\begin{aligned}\vec{R'}_i &= \vec{R}_i + \frac{1}{2}\vec{R}_{diff}, \\ \vec{R'}_j &= \vec{R}_j - \frac{1}{2}\vec{R}_{diff}.\end{aligned} \tag{4.20}$$

Next we propagate with the spin operator $\mathrm{e}^{-i\sqrt{\frac{mA\Delta t}{16\hbar^2}}[(\vec{\sigma}_i+\vec{\sigma}_j)\times\vec{r}_{ij}]\cdot\vec{x}_{ij}v'_{ls}(r_{ij})}$. The spin operators $\vec{\sigma}_i\times\vec{r}_{ij}$ and $\vec{\sigma}_j\times\vec{r}_{ij}$ will rotate the spinors $|s_i\rangle$ and $|s_j\rangle$ simultaneously.

$$|s'_i\rangle = \mathrm{e}^{-i\sqrt{\frac{mA\Delta t}{16\hbar^2}}[\vec{\sigma}_i\times\vec{r}_{ij}]\cdot\vec{x}_{ij}v'_{ls}(r_{ij})}|s_i\rangle, \tag{4.21}$$

$$|s'_j\rangle = \mathrm{e}^{-i\sqrt{\frac{mA\Delta t}{16\hbar^2}}[\vec{\sigma}_j\times\vec{r}_{ij}]\cdot\vec{x}_{ij}v'_{ls}(r_{ij})}|s_j\rangle. \tag{4.22}$$

Thus, we have used the Hubbard-Stratonovich method to linearise the spin-orbit propagators. The pair-wise propagation has been employed because we combined the spin-orbit with momentum operator, and the counter terms are easily included with the v6' potential part. The pair-wise propagation is equivalent to single-particle propagation, since it is simply a different linearization method.

4.2 Spin-Orbit Interactions in Nuclear Matter

In this section, we will calculate the spin-orbit interactions in nuclear matter. The Hamiltonian we are using is the same as for neutron matter in last section. The only

difference is that the isospin operator in $\vec{L}\cdot\vec{S}(\vec{\tau}_i\cdot\vec{\tau}_j)$ is not constant. It will rotate the isospin states of the nucleons correlated with the spin-orbit interactions. This makes it difficult to propagate $\vec{L}\cdot\vec{S}(\vec{\tau}_i\cdot\vec{\tau}_j)$ in nuclear matter, because there is now a 3-operator product to linearize.

The Hamiltonian is the same as equation 4.1. It could be written in a more specific way as the following.

$$\begin{aligned} H = &\sum_i \frac{p_i^2}{2m} + \sum_{i<j} v^c(r_{ij}) + \sum_{i<j,\alpha\beta} \{v^\sigma(r_{ij})\delta_{\alpha\beta} + v^t(r_{ij})[3\hat{\alpha}\cdot\hat{r}_{ij}\hat{\beta}\cdot\hat{r}_{ij} - \delta_{\alpha\beta}]\}\sigma_{i\alpha}\sigma_{j\beta} \\ &+ \sum_{i<j,\alpha\beta\gamma} \{v^{\sigma\tau(r_{ij})\delta_{\alpha\beta}} + v^{t\tau}(r_{ij})\}[3\hat{\alpha}\cdot\hat{r}_{ij}\hat{\beta}\cdot\hat{r}_{ij} - \delta_{\alpha\beta}][\sigma_{i\alpha}\tau_{i\gamma}][\sigma_{j\beta}\tau_{j\gamma}] \\ &+ \sum_{i<j,\gamma} v^\tau(r_{ij})\tau_{i\gamma}\tau_{j\gamma} + \sum_{i<j} \frac{1}{2\hbar}\{[(\vec{r}_i - \vec{r}_j)\times\vec{p}_{ij}]\cdot(\vec{\sigma}_i + \vec{\sigma}_j)\}[v_{ls}(r_{ij}) + \vec{\tau}_i\cdot\vec{\tau}_j v_{ls\tau}(r_{ij})]. \end{aligned} \tag{4.23}$$

The first six spin, isospin operators are treated as previously. We write the momentum-dependent terms as H_r, which only contains the spin-orbit interactions and kinetic energy.

$$H_r = \sum_{i<j}\left\{\frac{p_{ij}^2}{\frac{1}{2}mA} + \vec{p}_{ij}\cdot\frac{1}{2\hbar}[(\vec{\sigma}_i + \vec{\sigma}_j)\times\vec{r}_{ij}][v^{ls}(r_{ij}) + \vec{\tau}_i\cdot\vec{\tau}_j v^{ls\tau}(r_{ij})]\right\}. \tag{4.24}$$

This is the same as equation 4.8, except that now there is a $\vec{\tau}_i\cdot\vec{\tau}_j$ interaction combined with the in spin-orbit-isospin terms, which we must break up. We rewrite H_r as sum of three parts, which correspond to the three components of the isospin operator. The separation of the three components should reduce the variance since these isospin components commute and the commutator terms from the breakup are zero.

$$H_r = \sum_{i<j}\sum_{\alpha=1}^{3}\left\{\frac{p_{ij}^2}{\frac{3}{2}mA} + \vec{p}_{ij}\cdot\frac{1}{2\hbar}[(\vec{\sigma}_i + \vec{\sigma}_j)\times\vec{r}_{ij}][\frac{1}{3}v^{ls}(r_{ij}) + \tau_{i\alpha}\tau_{j\alpha}v^{ls\tau}(r_{ij})]\right\}. \tag{4.25}$$

As we did in last section, the equation above can be rewritten as:

$$\begin{aligned} H_r = &\sum_{i<j}\sum_{\alpha=1}^{3}\frac{2}{3mA}\left(\vec{p}_{ij}+\frac{3mA}{8\hbar}[(\vec{\sigma}_i+\vec{\sigma}_j)\times\vec{r}_{ij}][\frac{1}{3}v_{ls}(r_{ij})+\tau_{i\alpha}\tau_{j\alpha}v_{ls\tau}(r_{ij})]\right)^2 \\ &-\sum_{i<j}\sum_{\alpha=1}^{3}\frac{3mA}{32\hbar^2}[(\vec{\sigma}_i+\vec{\sigma}_j)\times\vec{r}_{ij}]^2[\frac{1}{3}v_{ls}(r_{ij})+\tau_{i\alpha}\tau_{j\alpha}v_{ls\tau}(r_{ij})]^2, \end{aligned} \tag{4.26}$$

where the counter term becomes:

$$v_{counter} = -\sum_{i<j}\sum_{\alpha=1}^{3}\frac{3mA}{32\hbar^2}[(\vec{\sigma}_i+\vec{\sigma}_j)\times\vec{r}_{ij}]^2[\frac{1}{3}v^{ls}(r_{ij})+\tau_{i\alpha}\tau_{j\alpha}v^{ls\tau}(r_{ij})]^2. \tag{4.27}$$

H_r now is a sum of squares of operators, so we can apply the Hubbard-Stratonovich transformation. The propagator becomes:

$$\begin{aligned} e^{-H_r\Delta t} = \prod_{\alpha,i<j}\frac{1}{(2\pi)^{\frac{3}{2}}}\int \mathrm{d}^3x_{ij\alpha}\mathrm{e}^{-\frac{|x_{ij\alpha}|^2}{2}}\mathrm{e}^{\frac{3mA\Delta t}{32\hbar^2}[(\vec{\sigma}_i+\vec{\sigma}_j)\times\vec{r}_{ij}]^2[\frac{1}{3}v_{ls}(r_{ij})+\tau_{i\alpha}\tau_{j\alpha}v_{ls\tau}(r_{ij})]^2} \\ \cdot\,\mathrm{e}^{-\frac{i}{\hbar}\sqrt{\frac{4\Delta t\hbar^2}{3mA}}\left(\vec{p}_{ij}+\frac{3mA}{8\hbar}[(\vec{\sigma}_i+\vec{\sigma}_j)\times\vec{r}_{ij}][\frac{1}{3}v_{ls}(r_{ij})+\tau_{i\alpha}\tau_{j\alpha}v_{ls\tau}(r_{ij})]\right)\cdot\vec{x}_{ij\alpha}}. \end{aligned} \tag{4.28}$$

The $v_{counter}$ in propagator 4.28 does not depend on the momentum operator. It can be moved out of the integral, and combined with the rest of the potential. $\vec{x}_{ij\alpha}$ is our first auxiliary field. Again, it can be sampled with importance sampling from

$$\vec{x}_{ij\alpha} = \vec{\chi}_{ij\alpha} - i\sqrt{\lambda_{ij\alpha}\Delta t}\langle\vec{O}_{ij\alpha}\rangle. \tag{4.29}$$

In this section, the values of $\lambda_{ij\alpha}$ and $\vec{O}_{ij\alpha}$ are:

$$\lambda_{ij\alpha} = \frac{4}{3mA}, \tag{4.30}$$

$$\vec{O}_{ij\alpha} = \vec{p}_{ij}+\frac{3mA}{8\hbar}[(\vec{\sigma}_i+\vec{\sigma}_j)\times\vec{r}_{ij}][\frac{1}{3}v^{ls}(r_{ij})+\tau_{i\alpha}\tau_{j\alpha}v^{ls\tau}(r_{ij})]. \tag{4.31}$$

So our first auxiliary field $x_{ij\alpha}$ is

$$\begin{aligned} \vec{x}_{ij\alpha} =&\vec{\chi}_{ij\alpha} - i\sqrt{\frac{4\Delta t}{3mA}}\langle\vec{p}_{ij\alpha}\rangle - i\sqrt{\frac{3mA\Delta t}{16\hbar^2}}\langle(\vec{\sigma}_i+\vec{\sigma}_j)\times\vec{r}_{ij}\rangle \\ &\cdot[\frac{1}{3}v_{ls}(r_{ij})+\langle\tau_{i\alpha}\tau_{j\alpha}\rangle v_{ls\tau}(r_{ij})]. \end{aligned} \tag{4.32}$$

Now we will use $\vec{O}_{ij\alpha}$ to simplify the right-hand side of equation 4.28. There are three terms in $\vec{O}_{ij\alpha}$: momentum, spin, and spin-isospin. The momentum and spin operators can be propagated by first auxiliary field $\vec{x}_{ij\alpha}$ as in last section, while the spin-isospin terms need to be broken up. This is the difficult part of the simulation of nuclear matter. Because we use the walker basis $|RS\rangle$, after propagation by one time step, it will become a new state $|R'S'\rangle$. But if there is product of spin operators in the propagator, it will produce 4^A spin basis states instead of $4A$ spin basis states we are using now. Since the exponent is not linear in the i and j particle operators, to solve this problem, we introduce a second auxiliary field to break up the spin-isospin interaction in equation 4.28. But before that, we need to propagate the momentum and spin operators in $\vec{O}_{ij\alpha}$ as we did in last section.

First, we propagate with the momentum operator $\mathrm{e}^{-\frac{i}{\hbar}\sqrt{\frac{4\Delta t\hbar^2}{3mA}}\vec{p}_{ij\alpha}\cdot\vec{x}_{ij\alpha}}$. Similarly as in equation 4.17, we have:

$$\vec{R'}_{ij} = \vec{R}_{ij} + \vec{x}_{ij\alpha}\sqrt{\frac{4\Delta t\hbar^2}{3mA}}. \tag{4.33}$$

Substituting (4.32) into (4.33), and using the fixed-phase approximation, we have

$$\begin{aligned}\vec{R'}_{ij} =& \vec{R}_{ij} + \vec{\chi}_{ij\alpha}\sqrt{\frac{4\Delta t\hbar^2}{3mA}} - \frac{4\Delta t\hbar}{3mA}\langle\vec{p}_{ij\alpha}\rangle \\ &- \mathrm{Re}\left[i\frac{\Delta t}{2}\langle(\vec{\sigma}_i+\vec{\sigma}_j)\times\vec{r}_{ij}\rangle[\frac{1}{3}v_{ls}(r_{ij}) + \langle\tau_{i\alpha}\tau_{j\alpha}\rangle v_{ls\tau}(r_{ij})]\right].\end{aligned} \tag{4.34}$$

We define the $\vec{R}_{diff}$ as

$$\begin{aligned}\vec{R}_{diff} =& \vec{\chi}_{ij\alpha}\sqrt{\frac{4\Delta t\hbar^2}{3mA}} - \frac{4\Delta t\hbar}{3mA}\langle\vec{p}_{ij\alpha}\rangle \\ &- \mathrm{Re}\left[i\frac{\Delta t}{2}\langle(\vec{\sigma}_i+\vec{\sigma}_j)\times\vec{r}_{ij}\rangle[\frac{1}{3}v_{ls}(r_{ij}) + \langle\tau_{i\alpha}\tau_{j\alpha}\rangle v_{ls\tau}(r_{ij})]\right].\end{aligned} \tag{4.35}$$

Thus the translations of the positions of one pair can be written as:

$$\begin{aligned}\vec{R'}_i &= \vec{R}_i + \frac{1}{2}\vec{R}_{diff}, \\ \vec{R'}_j &= \vec{R}_j - \frac{1}{2}\vec{R}_{diff}.\end{aligned} \tag{4.36}$$

Second, we propagate with the spin operator $\mathrm{e}^{-i\sqrt{\frac{3mA\Delta t}{16\hbar^2}}[(\vec{\sigma}_i+\vec{\sigma}_j)\times\vec{r}_{ij}]\cdot\vec{x}_{ij\alpha}\frac{1}{3}v_{ls}(r_{ij})}$. The spin operators $\vec{\sigma}_i \times \vec{r}_{ij}$ and $\vec{\sigma}_j \times \vec{r}_{ij}$ rotate the spinors $|s_i\rangle$ and $|s_j\rangle$ separately as in last section.

$$|s_i'\rangle = \mathrm{e}^{-i\sqrt{\frac{3mA\Delta t}{16\hbar^2}}[\vec{\sigma}_i\times\vec{r}_{ij}]\cdot\vec{x}_{ij\alpha}\frac{1}{3}v_{ls}(r_{ij})}|s_i\rangle, \tag{4.37}$$

$$|s_j'\rangle = \mathrm{e}^{-i\sqrt{\frac{3mA\Delta t}{16\hbar^2}}[\vec{\sigma}_j\times\vec{r}_{ij}]\cdot\vec{x}_{ij\alpha}\frac{1}{3}v_{ls}(r_{ij})}|s_j\rangle. \tag{4.38}$$

Lastly, we propagate the spin-isospin operator $\mathrm{e}^{-i\sqrt{\frac{3mA\Delta t}{16\hbar^2}}[(\vec{\sigma}_i+\vec{\sigma}_j)\times\vec{r}_{ij}]\cdot\vec{x}_{ij\alpha}\tau_{i\alpha}\tau_{j\alpha}v_{ls\tau}(r_{ij})}$, which needs to break up with a second auxiliary field. To simplify the expression, we rewrite the operator terms as

$$[(\vec{\sigma}_i + \vec{\sigma}_j) \times \vec{r}_{ij}] \cdot \vec{x}_{ij\alpha} = (\vec{\sigma}_i + \vec{\sigma}_j) \cdot (\vec{r}_{ij} \times \vec{x}_{ij\alpha}), \tag{4.39}$$

and define

$$\gamma = |\vec{r}_{ij} \times \vec{x}_{ij\alpha}| \left[-i\sqrt{\frac{3mA\Delta t}{16\hbar^2}} v^{ls\tau}(r_{ij}) \right], \tag{4.40}$$

$$\hat{\gamma} = \frac{\vec{r}_{ij} \times \vec{x}_{ij\alpha}}{|\vec{r}_{ij} \times \vec{x}_{ij\alpha}|}, \tag{4.41}$$

$$\sigma_{i\gamma} = \vec{\sigma}_i \cdot \hat{\gamma}, \tag{4.42}$$

$$\sigma_{j\gamma} = \vec{\sigma}_j \cdot \hat{\gamma}. \tag{4.43}$$

So the spin-isospin operator becomes

$$\mathrm{e}^{\gamma\tau_{i\alpha}\tau_{j\alpha}(\sigma_{i\gamma}+\sigma_{j\gamma})}. \tag{4.44}$$

Now we will rewrite the operator in 4.44 as a sum of squares, and apply a second Hubbard-Stratonovich transformation to break up the $\tau_{i\alpha}\tau_{j\alpha}$ interactions.

$$\begin{aligned}
\gamma\tau_{i\alpha}\tau_{j\alpha}(\sigma_{i\gamma} + \sigma_{j\gamma}) &= \gamma\sigma_{i\gamma}\tau_{i\alpha}\tau_{j\alpha} + \gamma\sigma_{j\gamma}\tau_{j\alpha}\tau_{i\alpha} \\
&= \gamma \left[\frac{(\sigma_{i\gamma}\tau_{i\alpha} + \tau_{j\alpha})^2 + (i(\sigma_{i\gamma}\tau_{i\alpha} - \tau_{j\alpha}))^2}{4} \right] \\
&\quad + \gamma \left[\frac{(\sigma_{j\gamma}\tau_{j\alpha} + \tau_{i\alpha})^2 + (i(\sigma_{j\gamma}\tau_{j\alpha} - \tau_{i\alpha}))^2}{4} \right].
\end{aligned} \tag{4.45}$$

Since the spin-isospin operators can all be written as a sum of squares, the propagator in 4.44 we can apply the Hubbard-Stratonovich transformation again,

$$\begin{aligned} &\mathrm{e}^{\gamma\left[\frac{(\sigma_{i\gamma}\tau_{i\alpha}+\tau_{j\alpha})^2+(i(\sigma_{i\gamma}\tau_{i\alpha}-\tau_{j\alpha})^2}{4}+\frac{(\sigma_{j\gamma}\tau_{j\alpha}+\tau_{i\alpha})^2+(i(\sigma_{j\gamma}\tau_{j\alpha}-\tau_{i\alpha}))^2}{4}\right]} \\ &= \frac{1}{(2\pi)^2}\int \mathrm{d}y_1\mathrm{d}y_2\mathrm{d}y_3\mathrm{d}y_4\mathrm{e}^{-\frac{y_1^2+y_2^2+y_3^2+y_4^2}{2}} \\ &\quad \cdot \mathrm{e}^{\sqrt{\frac{\gamma}{2}}\{y_1(\sigma_{i\gamma}\tau_{i\alpha}+\tau_{j\alpha})+iy_2(\sigma_{i\gamma}\tau_{i\alpha}-\tau_{j\alpha})+y_3(\sigma_{j\gamma}\tau_{j\alpha}+\tau_{i\alpha})+iy_4(\sigma_{j\gamma}\tau_{j\alpha}-\tau_{i\alpha})\}}. \end{aligned} \tag{4.46}$$

$\{y_1, y_2, y_3, y_4\}$ are the second auxiliary fields. By using importance sampling, they can be sampled as

$$y_1 = \chi_1 - \sqrt{\frac{\gamma}{2}}\left[\langle\sigma_{i\gamma}\tau_{i\alpha}\rangle + \langle\tau_{j\alpha}\rangle\right], \tag{4.47}$$

$$y_2 = \chi_2 - i\sqrt{\frac{\gamma}{2}}\left[\langle\sigma_{i\gamma}\tau_{i\alpha}\rangle - \langle\tau_{j\alpha}\rangle\right], \tag{4.48}$$

$$y_3 = \chi_3 - \sqrt{\frac{\gamma}{2}}\left[\langle\sigma_{j\gamma}\tau_{j\alpha}\rangle + \langle\tau_{i\alpha}\rangle\right], \tag{4.49}$$

$$y_4 = \chi_4 - i\sqrt{\frac{\gamma}{2}}\left[\langle\sigma_{j\gamma}\tau_{j\alpha}\rangle - \langle\tau_{i\alpha}\rangle\right]. \tag{4.50}$$

Where χ_1, χ_2, χ_3, and χ_4 are sampled from Gaussian distributions with unit variance. The coefficient γ is in order of $\sqrt{\Delta t}$, but it will not cause additional time step errors because if we integrate the spin-isospin operators via importance sampling, we will get the exact result of equation 4.44. So we can use the second auxiliary field to evaluate the spin-isospin operators. Finally, we propagate the spin-isospin operators as

$$|s_i'\rangle = \mathrm{e}^{\sqrt{\frac{\gamma}{2}}[(y_1+iy_2)\sigma_{i\gamma}\tau_{i\alpha}+(y_3-iy_4)\tau_{i\alpha}]}|s_i\rangle, \tag{4.51}$$

$$|s_j'\rangle = \mathrm{e}^{\sqrt{\frac{\gamma}{2}}[(y_1-iy_2)\tau_{j\alpha}+(y_3+iy_4)\sigma_{j\gamma}\tau_{j\alpha}]}|s_j\rangle. \tag{4.52}$$

To complete the integration in equation 4.28, we also need to integrate the counter terms of potential. Since the counter terms do not depend on momentum, we combine them with the V6' terms. The counter terms are:

$$V_{counter} = -\sum_{i<j}\sum_{\alpha=1}^{3}\frac{3mA}{32\hbar^2}[(\vec{\sigma}_i+\vec{\sigma}_j)\times\vec{r}_{ij}]^2[\frac{1}{3}v_{ls}(r_{ij}) + \tau_{i\alpha}\tau_{j\alpha}v_{ls\tau}(r_{ij})]^2, \tag{4.53}$$

where

$$\begin{aligned}[(\vec{\sigma}_i+\vec{\sigma}_j)\times\vec{r}_{ij}]^2 &= [\vec{\sigma}_i\times\vec{r}_{ij}+\vec{\sigma}_j\times\vec{r}_{ij}]\cdot[\vec{\sigma}_i\times\vec{r}_{ij}+\vec{\sigma}_j\times\vec{r}_{ij}]\\ &= (\vec{\sigma}_i\times\vec{r}_{ij})\cdot(\vec{\sigma}_i\times\vec{r}_{ij})+(\vec{\sigma}_i\times\vec{r}_{ij})\cdot(\vec{\sigma}_j\times\vec{r}_{ij})\\ &\quad+(\vec{\sigma}_j\times\vec{r}_{ij})\cdot(\vec{\sigma}_i\times\vec{r}_{ij})+(\vec{\sigma}_j\times\vec{r}_{ij})\cdot(\vec{\sigma}_j\times\vec{r}_{ij}),\end{aligned} \tag{4.54}$$

since

$$(\vec{\sigma}_i\times\vec{r}_{ij})\cdot(\vec{\sigma}_i\times\vec{r}_{ij}) = (\vec{\sigma}_j\times\vec{r}_{ij})\cdot(\vec{\sigma}_j\times\vec{r}_{ij}) = 2r^2, \tag{4.55}$$

$$(\vec{\sigma}_i\times\vec{r}_{ij})\cdot(\vec{\sigma}_j\times\vec{r}_{ij})+(\vec{\sigma}_j\times\vec{r}_{ij})\cdot(\vec{\sigma}_i\times\vec{r}_{ij}) = \frac{4}{3}r^2\vec{\sigma}_i\cdot\vec{\sigma}_j-\frac{2r^2}{3}(3\vec{\sigma}_i\cdot\hat{r}_{ij}\cdot\vec{\sigma}_j\cdot\hat{r}_{ij}-\vec{\sigma}_i\cdot\vec{\sigma}_j), \tag{4.56}$$

we have

$$[(\vec{\sigma}_i+\vec{\sigma}_j)\times\vec{r}_{ij}]^2 = 4r^2+\frac{4}{3}r^2\vec{\sigma}_i\cdot\vec{\sigma}_j-\frac{2r^2}{3}(3\vec{\sigma}_i\cdot\hat{r}_{ij}\cdot\vec{\sigma}_j\cdot\hat{r}_{ij}-\vec{\sigma}_i\cdot\vec{\sigma}_j). \tag{4.57}$$

Therefore,

$$\begin{aligned}V_{counter} =& -\sum_{i<j}\sum_{\alpha=1}^{3}\frac{3mA}{32\hbar^2}[4r^2+\frac{4}{3}r^2\vec{\sigma}_i\cdot\vec{\sigma}_j-\frac{2r^2}{3}(3\vec{\sigma}_i\cdot\hat{r}_{ij}\cdot\vec{\sigma}_j\cdot\hat{r}_{ij}-\vec{\sigma}_i\cdot\vec{\sigma}_j)]\\ &[\frac{1}{9}(v_{ls})^2+(v_{ls\tau})^2+\frac{2}{3}\tau_{i\alpha}\tau_{j\alpha}v_{ls}v_{ls\tau}]\\ =& -\sum_{ij}\frac{3mA}{32\hbar^2}[4r^2+\frac{4}{3}r^2\vec{\sigma}_i\cdot\vec{\sigma}_j-\frac{2r^2}{3}(3\vec{\sigma}_i\cdot\hat{r}_{ij}\cdot\vec{\sigma}_j\cdot\hat{r}_{ij}-\vec{\sigma}_i\cdot\vec{\sigma}_j)]\\ &[\frac{1}{3}(v_{ls})^2+3(v_{ls\tau})^2+\frac{2}{3}\vec{\tau}_i\cdot\vec{\tau}_jv_{ls}v_{ls\tau}].\end{aligned} \tag{4.58}$$

Now the potential counter terms contain only spin and isospin operators, so they are combined with the first six spin isospin operators, giving

central:

$$-\frac{3mA}{32\hbar^2}[4r^2][\frac{1}{3}(v_{ls})^2+3(v_{ls\tau})^2], \tag{4.59}$$

isospin:

$$-\frac{3mA}{32\hbar^2}[4r^2][\frac{2}{3}\vec{\tau}_i\cdot\vec{\tau}_jv_{ls}v_{ls\tau}], \tag{4.60}$$

spin:

$$-\frac{3mA}{32\hbar^2}[\frac{4}{3}r^2\vec{\sigma}_i\cdot\vec{\sigma}_j-\frac{2r^2}{3}(3\vec{\sigma}_i\cdot\hat{r}_{ij}\cdot\vec{\sigma}_j\cdot\hat{r}_{ij}-\vec{\sigma}_i\cdot\vec{\sigma}_j)][\frac{1}{3}(v_{ls})^2+3(v_{ls\tau})^2], \tag{4.61}$$

spin-isospin:

$$-\frac{3mA}{32\hbar^2}[\frac{4}{3}r^2\vec{\sigma}_i\cdot\vec{\sigma}_j-\frac{2r^2}{3}(3\vec{\sigma}_i\cdot\hat{r}_{ij}\cdot\vec{\sigma}_j\cdot\hat{r}_{ij}-\vec{\sigma}_i\cdot\vec{\sigma}_j)][\frac{2}{3}\vec{\tau}_i\cdot\vec{\tau}_j v_{ls}v_{ls\tau}]. \tag{4.62}$$

The above four counter term potentials and the propagator of equation 4.28 completes the propagation of Hamiltonian with Argonne v8'. Since they cancel, the counter terms in above four potentials are not included for the calculation of local energy.

In summary, we use Hubbard-Stratonovich transformation to linearize the operators in the Hamiltonian to form the propagator and use a local-energy weight in each propagation. The spin-orbit interactions are combined with the momentum operator in the propagator, leaving the counter terms which are combined with the v6 potential operators. We branch on the weight. Therefore the trial wave function can be diffused to the ground-state wave function within the fixed-phase constraint.

4.3 Variance in Spin-Orbit Variables

By using the Hubbard-Stratonovich method twice, with a first and second auxiliary field, we can successfully include the spin-orbit with isospin interactions in nuclear matter. Though the propagator in equation 4.46 for a second auxiliary field is of order $\sqrt{\Delta t}$, there is no extra time step error after integration.

However, since the shifted Gaussian sampling is not totally symmetric, there is variance from sampling for the second auxiliary field. To reduce the variance, we expand the propagator to develop correlated sampling to lower the variance. We

rewrite the spin-isospin propagator in equation 4.46 as

$$\frac{1}{(2\pi)^2}\int \mathrm{d}y_1\mathrm{d}y_2\mathrm{d}y_3\mathrm{d}y_4\mathrm{e}^{-\frac{y_1^2+y_2^2+y_3^2+y_4^2}{2}} \cdot \mathrm{e}^{\sqrt{\frac{\gamma}{2}}\{y_1(\sigma_{i\gamma}\tau_{i\alpha}+\tau_{j\alpha})+iy_2(\sigma_{i\gamma}\tau_{i\alpha}-\tau_{j\alpha})+y_3(\sigma_{j\gamma}\tau_{j\alpha}+\tau_{i\alpha})+iy_4(\sigma_{j\gamma}\tau_{j\alpha}-\tau_{i\alpha})\}}, \tag{4.63}$$

where $\gamma = |\vec{r}_{ij}\times\vec{x}|\left[-i\sqrt{\frac{3mA\Delta t}{16\hbar^2}}v_{ls\tau}\right]$. Then expand the integrand

$$\begin{aligned}
&\mathrm{e}^{\sqrt{\frac{\gamma}{2}}\{y_1(\sigma_{i\gamma}\tau_{i\alpha}+\tau_{j\alpha})+iy_2(\sigma_{i\gamma}\tau_{i\alpha}-\tau_{j\alpha})+y_3(\sigma_{j\gamma}\tau_{j\alpha}+\tau_{i\alpha})+iy_4(\sigma_{j\gamma}\tau_{j\alpha}-\tau_{i\alpha})\}}\\
=&1+\sqrt{\frac{\gamma}{2}}\{y_1(\sigma_{i\gamma}\tau_{i\alpha}+\tau_{j\alpha})+iy_2(\sigma_{i\gamma}\tau_{i\alpha}-\tau_{j\alpha})+y_3(\sigma_{j\gamma}\tau_{j\alpha}+\tau_{i\alpha})+iy_4(\sigma_{j\gamma}\tau_{j\alpha}-\tau_{i\alpha})\}\\
&+\frac{1}{2}(\frac{\gamma}{2})\{y_1(\sigma_{i\gamma}\tau_{i\alpha}+\tau_{j\alpha})+iy_2(\sigma_{i\gamma}\tau_{i\alpha}-\tau_{j\alpha})+y_3(\sigma_{j\gamma}\tau_{j\alpha}+\tau_{i\alpha})+iy_4(\sigma_{j\gamma}\tau_{j\alpha}-\tau_{i\alpha})\}^2\\
&+\frac{1}{6}(\frac{\gamma}{2})^{\frac{3}{2}}\{y_1(\sigma_{i\gamma}\tau_{i\alpha}+\tau_{j\alpha})+iy_2(\sigma_{i\gamma}\tau_{i\alpha}-\tau_{j\alpha})+y_3(\sigma_{j\gamma}\tau_{j\alpha}+\tau_{i\alpha})+iy_4(\sigma_{j\gamma}\tau_{j\alpha}-\tau_{i\alpha})\}^3\\
&+\frac{1}{24}(\frac{\gamma}{2})^2\{y_1(\sigma_{i\gamma}\tau_{i\alpha}+\tau_{j\alpha})+iy_2(\sigma_{i\gamma}\tau_{i\alpha}-\tau_{j\alpha})+y_3(\sigma_{j\gamma}\tau_{j\alpha}+\tau_{i\alpha})+iy_4(\sigma_{j\gamma}\tau_{j\alpha}-\tau_{i\alpha})\}^4\\
&+\ldots .
\end{aligned} \tag{4.64}$$

In equation 4.46, we wish to use correlated sampling to calculate the variance from $\{y_1, y_2, y_3, y_4\}$, which is lower order than Δt.

For the terms in $\sqrt{\frac{\gamma}{2}}$ and $\frac{1}{6}(\frac{\gamma}{2})^{\frac{3}{2}}$, the variance from $\{+y_1, +y_2, +y_3, +y_4\}$ can be cancelled by also including $\{-y_1, -y_2, -y_3, -y_4\}$. So instead of one set of second auxiliary fields, we use two sets, the initially sampled y and negative of y to cancel the variance of order of $(\Delta t)^{\frac{1}{4}}$ and $(\Delta t)^{\frac{3}{4}}$.

For the terms in $\frac{1}{2}(\frac{\gamma}{2})$ and $\frac{1}{24}(\frac{\gamma}{2})^2$, if the $\frac{1}{2}(\frac{\gamma}{2})$ term's variance is cancelled, the $\frac{1}{24}(\frac{\gamma}{2})^2$ term's variance is cancelled too. So we need to eliminate the variance in $\frac{1}{2}(\frac{\gamma}{2})$

term. Expanding it,

$$\begin{aligned}
&\frac{1}{2}(\frac{\gamma}{2})\left\{y_1(\sigma_{i\gamma}\tau_{i\alpha}+\tau_{j\alpha})+iy_2(\sigma_{i\gamma}\tau_{i\alpha}-\tau_{j\alpha})+y_3(\sigma_{j\gamma}\tau_{j\alpha}+\tau_{i\alpha})+iy_4(\sigma_{j\gamma}\tau_{j\alpha}-\tau_{i\alpha})\right\}^2 \\
&= 2(y_1^2-y_2^2)+(y_1^2+y_2^2)2\sigma_{i\gamma}\tau_{i\alpha}\tau_{j\alpha}+2(y_3^2-y_4^2)+(y_3^2+y_4^2)2\sigma_{j\gamma}\tau_{j\alpha}\tau_{i\alpha} \\
&\quad + 2y_1y_3(\sigma_{i\gamma}\tau_{i\alpha}+\tau_{j\alpha})(\sigma_{j\gamma}\tau_{j\alpha}+\tau_{i\alpha})+2iy_1y_4(\sigma_{i\gamma}\tau_{i\alpha}+\tau_{j\alpha})(\sigma_{j\gamma}\tau_{j\alpha}-\tau_{i\alpha}) \\
&\quad\quad + 2iy_2y_3(\sigma_{i\gamma}\tau_{i\alpha}-\tau_{j\alpha})(\sigma_{j\gamma}\tau_{j\alpha}+\tau_{i\alpha})-2y_2y_4(\sigma_{i\gamma}\tau_{i\alpha}-\tau_{j\alpha})(\sigma_{j\gamma}\tau_{j\alpha}-\tau_{i\alpha}).
\end{aligned} \tag{4.65}$$

Since $\gamma \sim \sqrt{\Delta t}$, any variance from formula 4.65 would increase the variance as $\Delta t \to 0$ faster than the signal, which goes like Δt. All the terms on the right-hand side of the equation should integrate to zero. One thing need to be paid attention to is that there is the first auxiliary field $\vec{x}_{ij\alpha}$ in the formula as well. From definitions 4.40 to 4.43:

$$\gamma = |\vec{r}_{ij}\times\vec{x}_{ij\alpha}|\left[-i\sqrt{\frac{3mA\Delta t}{16\hbar^2}}v^{ls\tau}(r_{ij})\right], \tag{4.66}$$

$$\hat{\gamma} = \frac{\vec{r}_{ij}\times\vec{x}_{ij\alpha}}{|\vec{r}_{ij}\times\vec{x}_{ij\alpha}|}, \tag{4.67}$$

$$\sigma_{i\gamma} = \vec{\sigma}_i\cdot\hat{\gamma}, \tag{4.68}$$

$$\sigma_{j\gamma} = \vec{\sigma}_j\cdot\hat{\gamma}. \tag{4.69}$$

We can see that when we change the sign of $\vec{x}_{ij\alpha}$, the sign of $\sigma_{i\gamma}$ and $\sigma_{j\gamma}$ also changes. So we can use sets $+\vec{x}_{ij\alpha}$ and $-\vec{x}_{ij\alpha}$ instead of $\vec{x}_{ij\alpha}$. There are also other ways, but the more correlations the sample sets of variables there are, the longer the calculation time, so we want the smallest number of sets possible.

Now there are six terms left on the right-hand side of equation 4.65. We work on

the following four terms first:

$$2y_1y_3(\sigma_{i\gamma}\tau_{i\alpha}+\tau_{j\alpha})(\sigma_{j\gamma}\tau_{j\alpha}+\tau_{i\alpha}),$$
$$2iy_1y_4(\sigma_{i\gamma}\tau_{i\alpha}+\tau_{j\alpha})(\sigma_{j\gamma}\tau_{j\alpha}-\tau_{i\alpha}),$$
$$2iy_2y_3(\sigma_{i\gamma}\tau_{i\alpha}-\tau_{j\alpha})(\sigma_{j\gamma}\tau_{j\alpha}+\tau_{i\alpha}),$$
$$-2y_2y_4(\sigma_{i\gamma}\tau_{i\alpha}-\tau_{j\alpha})(\sigma_{j\gamma}\tau_{j\alpha}-\tau_{i\alpha}).$$

It is not difficult to see that if the sign of y_iy_j changes, where $i=1,2$, $j=3,4$, the variance will be cancelled. So we use the following variables

$$\begin{pmatrix} +x & +y1 & +y2 & +y3 & +y4 \\ +x & +y1 & +y2 & -y3 & -y4 \\ +x & -y1 & -y2 & -y3 & -y4 \\ +x & -y1 & -y2 & +y3 & +y4 \end{pmatrix}, \tag{4.70}$$

and

$$\begin{pmatrix} -x & +y1 & +y2 & +y3 & +y4 \\ -x & +y1 & +y2 & -y3 & -y4 \\ -x & -y1 & -y2 & -y3 & -y4 \\ -x & -y1 & -y2 & +y3 & +y4 \end{pmatrix}. \tag{4.71}$$

For the last two terms in equation 4.65: $2(y_1^2-y_2^2)$ and $2(y_3^2-y_4^2)$, the order of y_1 and y_2 needs to be exchanged to cancel the variance in the first term. So do the y_3 and y_4. Therefore, there are 16 sets of variables to cancel the variance in the second

auxiliary field. They are 8 variables of

$$\begin{pmatrix} +x & +y1 & +y2 & +y3 & +y4 \\ +x & +y1 & +y2 & -y3 & -y4 \\ +x & -y1 & -y2 & -y3 & -y4 \\ +x & -y1 & -y2 & +y3 & +y4 \\ -x & +y1 & +y2 & +y3 & +y4 \\ -x & +y1 & +y2 & -y3 & -y4 \\ -x & -y1 & -y2 & -y3 & -y4 \\ -x & -y1 & -y2 & +y3 & +y4 \end{pmatrix}, \tag{4.72}$$

and 8 variables of:

$$\begin{pmatrix} +x & +y2 & +y1 & +y4 & +y3 \\ +x & +y2 & +y1 & -y4 & -y3 \\ +x & -y2 & -y1 & -y4 & -y3 \\ +x & -y2 & -y1 & +y4 & +y3 \\ -x & +y2 & +y1 & +y4 & +y3 \\ -x & +y2 & +y1 & -y4 & -y3 \\ -x & -y2 & -y1 & -y4 & -y3 \\ -x & -y2 & -y1 & +y4 & +y3 \end{pmatrix}. \tag{4.73}$$

Now we plot some figures to show that 16 sets of variables can cancel all the variance at orders lower than Δt and it is the minimum number of sets of variables needed. It is better to choose a simple system to check the variance. So we use 1 walker, 1 time-step propagation for 2 nucleons. If the variance in equation 4.64 could all be cancelled, the weight of one time-step propagation should be linear with Δt, since our error terms are order of Δt^2. The weight of one time-step propagation is the ratio of $\langle \Psi_T | R'S' \rangle$ over $\langle \Psi_T | RS \rangle$, where $|R'S'\rangle$ is a sampled propagation of $|RS\rangle$.

In the following figures we plot the weight versus time step for the 8 sets of

variables, and the weight versus time step for the 16 sets of variables. From the plotting we can see that, when we use 16 sets of variables, the line is linear. When we use 8 sets of variables, the variance increases at order of $\sqrt{\Delta t}$ with time step decreases. So as expected from the mathematics, 16 sets of variables are necessary to get a low-variance result using this method of 'antithetic' variables.

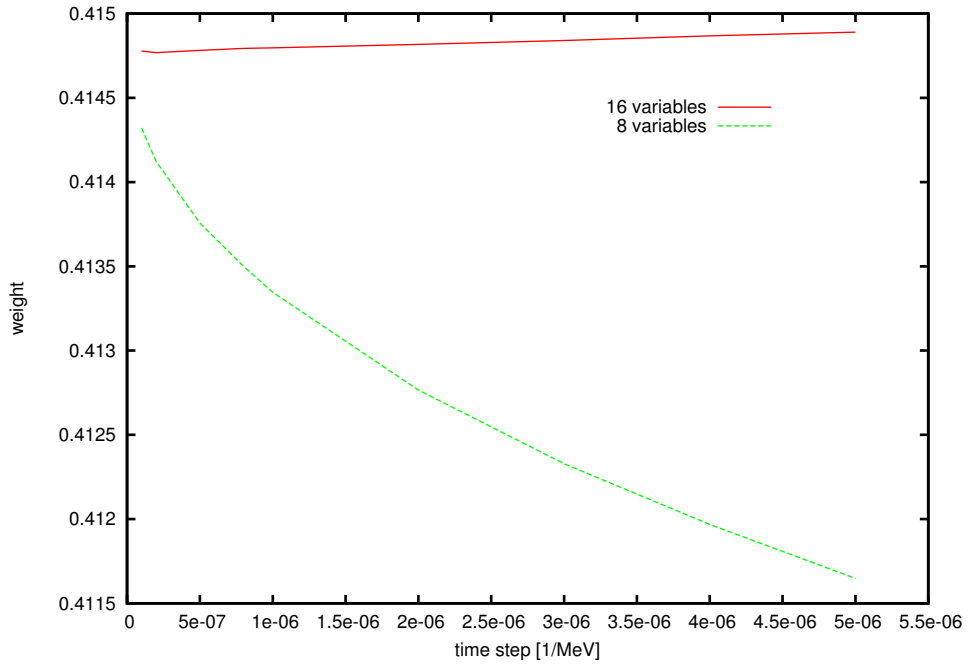

Figure 4.1: Variances with Different Sets of Variables When Using the Method of Antithetic Variables to Sample the Isospin-Dependent Spin-Orbit Interactions.

Chapter 5

RESULTS WITH THE FIRST AUXILIARY FIELD

In chapter 4, an auxiliary field was introduced to deal with the spin-orbit interactions in nuclear matter[97]. The spin-orbit interactions in Argonne v8' have two terms: spin-orbit without isospin $\vec{L}\cdot\vec{S}$, and spin-orbit with isospin $\vec{L}\cdot\vec{S}(\vec{\tau}_i\cdot\vec{\tau}_j)$. These two terms could be combined with kinetic energy, and re-written as sums of squares. The $\vec{L}\cdot\vec{S}$ could have been broken up by the first auxiliary field in the same way as Argonne v6'. But for the $\vec{L}\cdot\vec{S}(\vec{\tau}_i\cdot\vec{\tau}_i)$ term, since it is the product of three operators, it needs a second auxiliary field to linearize the operators. In this chapter, we will present the result of $\vec{L}\cdot\vec{S}$ with the first auxiliary field and the new pair-wise propagator. The results of $\vec{L}\cdot\vec{S}(\vec{\tau}_i\cdot\vec{\tau}_i)$ using the additional auxiliary field will be presented in next chapter.

From last chapter, we see that both the shifted Gaussian and the antithetic variables $\{\pm\vec{x}_{ij\alpha}, \pm\{y_1, y_2, y_3, y_4\}\}$ can be used for sampling. Either of them works for spin-orbit without isospin, but for spin-orbit with isospin, we can only use the latter one because of large time step errors. In this chapter, we will mainly use the antithetic sampling.

5.1 Checking the Pair-Wise Propagation

In section 4.1, the pair-wise propagation was developed for $\vec{L}\cdot\vec{S}$ in Argonne v8'. The previous simulations of Argonne v6' used single-particle propagation. These two methods are equivalent. Though the single-particle propagation could be used for $\vec{L}\cdot\vec{S}$

as well, we developed pair-wise propagation because it is necessary for the $\vec{L} \cdot \vec{S}(\vec{\tau}_i \cdot \vec{\tau}_j)$ term. We have used the two different propagation methods to simulate Argonne v6'. The following tables show that the results from pair-wise propagation agrees within error with single-particle propagation.

The test is for a 2-nucleon system with density $\rho = 0.16 fm^{-3}$, time step $\Delta t = 0.00001 MeV^{-1}$.

(1) Checking the kinetic energy and central force.

Table 5.1: Pair-Wise Propagation for Central Force

	mean value(MeV)	error bar(MeV)
single-particle propagation	-18.37	0.43
pair-wise propagation	-18.92	0.61

(2) Checking the Hamiltonian with Argonne v6'.

Table 5.2: Pair-Wise Propagation for Argonne v6'

	mean value(MeV)	error bar(MeV)
single-particle propagation	-14.93	0.64
pair-wise propagation	-14.91	0.69

From above two tables, we can see that the results of single-particle propagation agrees with the result of pair-wise propagation in Argonne v6'. It shows that we can use the latter method instead.

5.2 Checking the Spin-Orbit Propagator

From section 4.1, we know that the spin-orbit and kinetic energy part can be written as:

$$e^{-H_r\Delta t} = \prod_{i<j,\alpha=1,3} \frac{1}{(2\pi)^{\frac{3}{2}}} \int \mathrm{d}^3x_{ij\alpha} \mathrm{e}^{-\frac{|\vec{x}_{ij\alpha}|^2}{2}} \mathrm{e}^{-\frac{i}{\hbar}\sqrt{\frac{4\hbar^2\Delta t}{mA}}\left(\vec{p}_{ij}+\frac{mA}{8\hbar}[(\vec{\sigma}_i+\vec{\sigma}_j)\times\vec{r}_{ij}](v_{ls}(r_{ij}))\right)\cdot\vec{x}_{ij\alpha}} \cdot \mathrm{e}^{\frac{mA\Delta t}{32\hbar^2}[(\vec{\sigma}_i+\vec{\sigma}_j)\times\vec{r}_{ij}]^2(v_{ls}(r_{ij}))^2}. \tag{5.1}$$

In equation 5.1, there are two pieces: the propagator $e^{-\frac{i}{\hbar}\sqrt{\frac{4\hbar^2\Delta t}{mA}}\left(\vec{p}_{ij}+\frac{mA}{8\hbar}[(\vec{\sigma}_i+\vec{\sigma}_j)\times\vec{r}_{ij}](v_{ls}(r_{ij}))\right)\cdot\vec{x}_{ij}}$ changes the $|RS\rangle$ to $|R'S'\rangle$, while the counter term $e^{\frac{mA\Delta t}{32\hbar^2}[(\vec{\sigma}_i+\vec{\sigma}_j)\times\vec{r}_{ij}]^2(v_{ls}(r_{ij}))^2}$ is combined with Argonne v6'. These two pieces complete $e^{-H_r\Delta t}$.

In order to test the propagator $e^{-H_r\Delta t}$, we calculate the two pieces separately for one time-step propagation. By setting the momentum $\vec{p}_{ij}$ equal to zero, we have the mixed spin-orbit energy:

$$\prod_{i<j} \frac{1}{(2\pi)^{\frac{3}{2}}} \frac{\langle\Psi_T|\int \mathrm{d}^3x_{ij} \mathrm{e}^{-\frac{|\vec{x}_{ij}|^2}{2}} \mathrm{e}^{-\frac{i}{\hbar}\sqrt{\frac{4\hbar^2\Delta t}{mA}}\left(\frac{mA}{8\hbar}[(\vec{\sigma}_i+\vec{\sigma}_j)\times\vec{r}_{ij}](v_{ls}(r_{ij}))\right)\cdot\vec{x}_{ij}}|RS\rangle}{\langle\Psi_T|RS\rangle}. \tag{5.2}$$

It should have the same value of mixed energy as the counter term in equation 5.1, but with opposite sign. The mixed energy of counter term is:

$$\frac{\langle\Psi_T|\mathrm{e}^{\frac{mA\Delta t}{32\hbar^2}[(\vec{\sigma}_i+\vec{\sigma}_j)\times\vec{r}_{ij}]^2(v_{ls}(r_{ij}))^2}|RS\rangle}{\langle\Psi_T|RS\rangle}. \tag{5.3}$$

Equations 5.2 and 5.3 are different ways to calculate the spin-orbit mixed energy for one time-step propagation. They should be the same value but opposite sign. We checked this for 28 nucleons, including 14 protons and 14 neutrons. The number 28 is the first closed shell in the periodic box: 7 states of momentum($\vec{k} = \{0,0,0\}$, $\vec{k} = \{\pm1,0,0\}$, $\vec{k} = \{0,\pm1,0\}$, $\vec{k} = \{0,0,\pm1\}$), 4 states of spinors($p\uparrow, p\downarrow, n\uparrow, n\downarrow$). We chose the density as $\rho = 0.48fm^{-3}$; it is the highest density typically calculated

in our equation of state. The results of formula 5.2 and 5.3 are as follows.

Table 5.3: Mixed Energy of Spin-Orbit

mixed energy	mean value(MeV)	error bar(MeV)
propagator in 5.2	487.83	0.55
counter term in 5.3	-488.03	0.46

So equations 5.2 and 5.3 agree within statistical errors.

5.3 Checking the Variance

In chapter 3, we saw when the propagation time $t \to \infty$, the trial wave function propagates to the ground-state wave function. The total t is divided into many small time steps Δt. For each time step, the Hamiltonian is separated as kinetic energy and potential energy. The kinetic energy part diffuses the walkers, while the potential energy part branches the spinors, and the change of weight is sampled by branching. The kinetic energy does not commute with the potential, nor do the different spin operators, so there is time step error for each time step. The error is of order of Δt^2. Our desired result is the order Δt.

To check that there are no variance terms of lower order in our simulation, for each time step, we plot the ratio of new wave function over old wave function versus Δt. It should be a linear line, since our result is in order of Δt.

We first check one component in equation 5.1. The y-axis in figure 5.1 is the ratio of new wave function over old wave function, and the x-axis is the time step. We could see that the ratio is linear, as we expected.

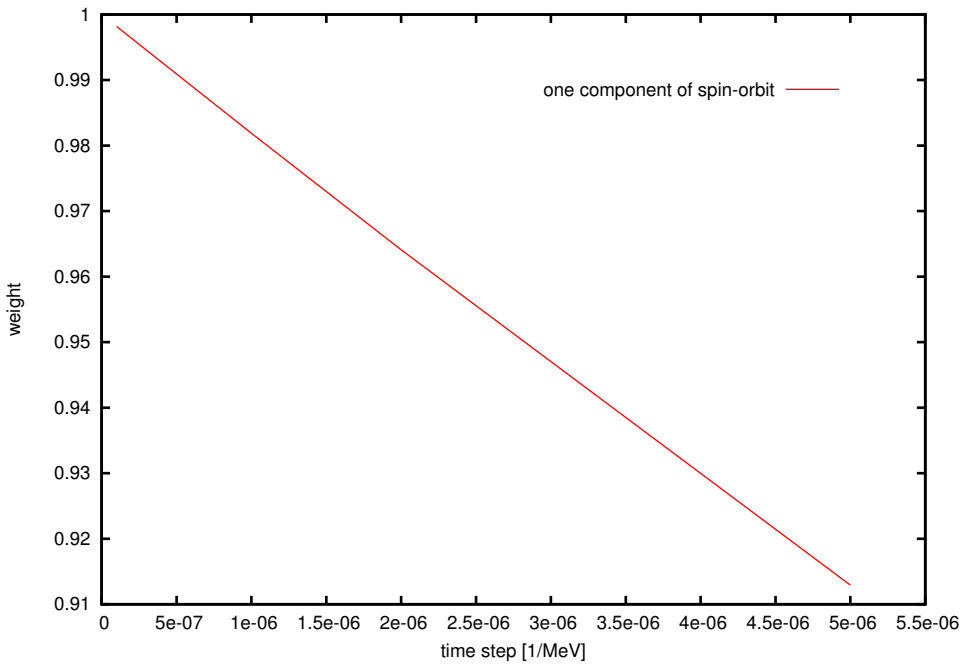

Figure 5.1: Variance Time Step Check for One Component of the Spin-Orbit Propagator. Linear Behavior Shows the Variance Terms Have Been Removed.

Next we check the three components of equation 5.1. The three α components in 5.1 are independent, so there should be no variance between them. The plot is shown in figure 5.2.

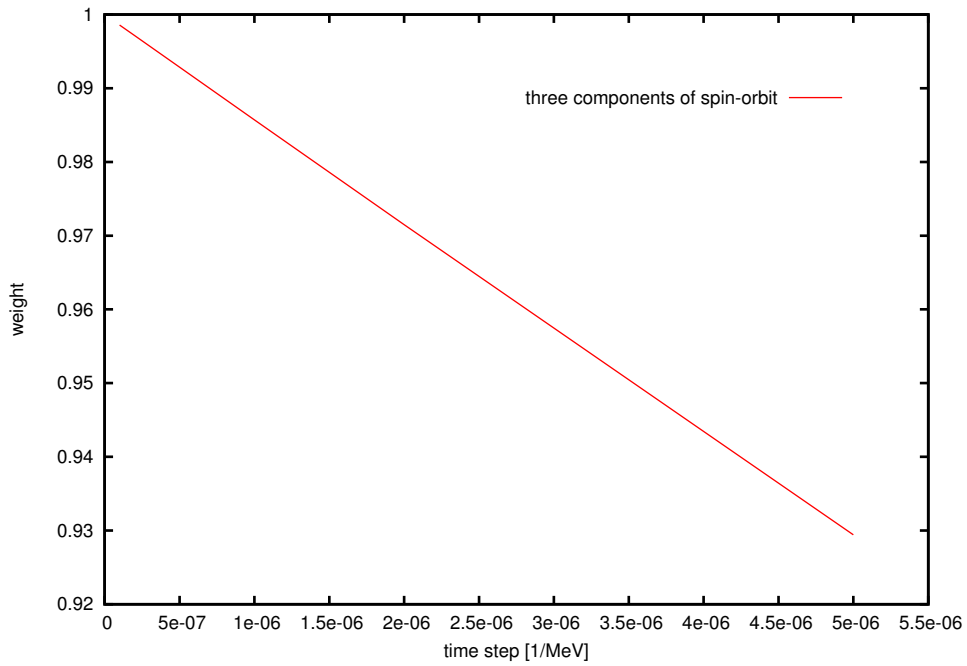

Figure 5.2: Same as Fig. 5.1 with Three Components of the Spin-Orbit Propagator.

The two figures above show that, for each time step propagation, there is no variance greater than order of Δt.

5.4 Results of Spin-Orbit without Isospin

In this chapter, we include the $\vec{L} \cdot \vec{S}$ interaction in the Hamiltonian. It could be combined with kinetic energy and sampled by auxiliary field with the Hubbard-Stratonovich transformation. Thus we have calculated the first seven operators in Argonne v8'; we call it v7 here. We still choose to calculate the 28 nucleons in nuclear matter to simulate the ground-state energy. The results of v7 and the previous results of v6 are listed in table 5.4.

The spin-orbit interaction is attractive force in nuclear matter, so it should decrease the ground-state energy. Table 5.4 shows that the ground-state energy in v7

Table 5.4: AFDMC in v6 and v7

$\rho(fm^{-3})$	AFDMC in v6 (MeV)	AFDMC in v7(MeV)
0.08	-7.31	-8.3
0.16	-11.97	-14.80
0.24	-15.02	-17.62
0.32	-15.62	-17.50
0.40	-13.01	-15.67
0.48	-10.99	-12.12

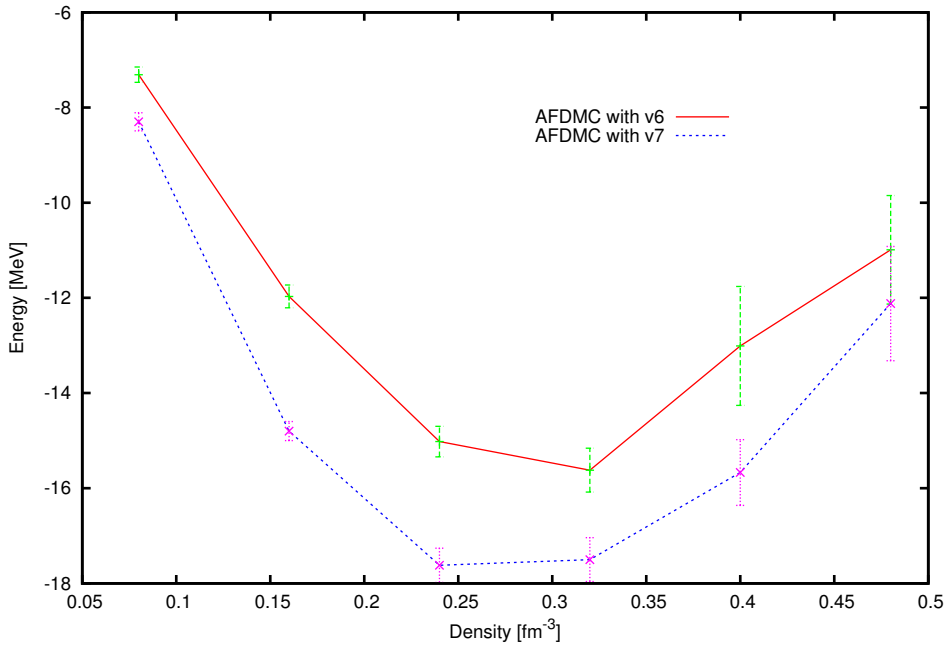

Figure 5.3: AFDMC in v7

is less than the one in v6, as we expected. In figure 5.3, we plot the ground state energies in both v6 and v7. They behave in a similar way. The gap between two lines is the effect of spin-orbit interaction without isospin in nuclear matter.

Chapter 6

RESULTS WITH THE SECOND AUXILIARY FIELD

In previous chapters, the Hubbard-Stratonovich transformation has been employed twice, giving two auxiliary fields to break up the the product of three operators $\vec{L} \cdot \vec{S}(\vec{\tau}_i \cdot \vec{\tau}_j)$, without causing additional time step error, and controlling the variance. In section 4.3, we showed how to use antithetic variables to eliminate variances of order less than Δt. So we use antithetic variables $\{\pm\vec{x}_{ij\alpha}, \pm\{y_1, y_2, y_3, y_4\}\}$ to sample the auxiliary fields.

In this chapter, we will show the results for the $\vec{L} \cdot \vec{S}(\vec{\tau}_i \cdot \vec{\tau}_j)$ interaction, and compare the results with some analytical results to show they are correctly calculated. Though the variance is eliminated mathematically, there can be round-off error when the time step is very small. All diffusion Monte Carlos require an extrapolation of the time step $\Delta t \to 0$ to get an accurate result. The initial work on this is complete. After this has been done, we will use Lanczos algorithm to check the spin-orbit interactions. The Lanczos algorithm developed for this is described in appendix A.

6.1 Checking the Spin-Orbit-Isospin Propagator

There are both first and second auxiliary fields in the spin-orbit with isospin propagator. In section 5.2, the propagator has been checked by calculating the mixed energy for one step of propagation. This method is used in this section as well. Since the spin-orbit with isospin is product of three operators, they need to be checked step by step.

We first fix the first auxiliary field, and calculate the $\frac{\langle\Psi_T|R'S'\rangle}{\langle\Psi_T|RS\rangle}$ with Monte Carlo analytically. The propagation equation is

$$\begin{aligned}
&\mathrm{e}^{\gamma\sigma_{i\gamma}\tau_{i\alpha}\tau_{j\alpha}+\gamma\sigma_{j\gamma}\tau_{j\alpha}\tau_{i\alpha}} \\
&= \frac{1}{(2\pi)^2}\int \mathrm{d}y_1\mathrm{d}y_2\mathrm{d}y_3\mathrm{d}y_4\mathrm{e}^{-\frac{y_1^2+y_2^2+y_3^2+y_4^2}{2}} \\
&\quad \cdot \mathrm{e}^{\sqrt{\frac{\gamma}{2}}\{y_1(\sigma_{i\gamma}\tau_{i\alpha}+\tau_{j\alpha})+iy_2(\sigma_{i\gamma}\tau_{i\alpha}-\tau_{j\alpha})+y_3(\sigma_{j\gamma}\tau_{j\alpha}+\tau_{i\alpha})+iy_4(\sigma_{j\gamma}\tau_{j\alpha}-\tau_{i\alpha})\}},
\end{aligned} \tag{6.1}$$

where $\gamma = |\vec{r}_{ij}\times\vec{x}|\left[-i\sqrt{\frac{3mA\Delta t}{16\hbar^2}}v_{ls\tau}\right]$. We fixed $\vec{x}_{ij\alpha}$ as $[1,1,1]$. The analytical result can be calculated for two particles. The comparisons between the analytic and simulation results are as follows.

(1) Results of the second auxiliary field y_1 with $\vec{x}_{ij\alpha}$ fixed.

$$\frac{\langle\Psi_T|e^{\frac{\gamma}{4}(\sigma_{i\gamma}\tau_{i\alpha}+\tau_{j\alpha})^2}|RS\rangle}{\langle\Psi_T|RS\rangle} = \frac{\langle\Psi_T|\int \mathrm{d}y_1\mathrm{e}^{-\frac{y_1^2}{2}}\mathrm{e}^{\sqrt{\frac{\gamma}{2}}y_1(\sigma_{i\gamma}\tau_{i\alpha}+\tau_{j\alpha})}|RS\rangle}{\langle\Psi_T|RS\rangle}. \tag{6.2}$$

The analytical result of the left-hand side of equation 6.2 is calculated by using a Taylor expansion for Δt. The right-hand side is a statistical result by using Gaussian sampling of y_1 for the same $|RS\rangle$. The Monte Carlo result agreed with the analytical result for a chosen $\Delta t = 1\times10^{-6}MeV^{-1}$.

Analytical result: $0.999\ 327\ 10(MeV)$

Monte Carlo result: $0.999\ 326\ 98(MeV)\pm 2.3\times10^{-7}(MeV)$

So the analytical result agrees with the Monte Carlo result.

(2) Results of the second auxiliary field y_2 with $\vec{x}_{ij\alpha}$ fixed. $\Delta t = 1\times10^{-6}MeV^{-1}$.

$$\frac{\langle\Psi_T|e^{-\frac{\gamma}{4}(\sigma_{i\gamma}\tau_{i\alpha}-\tau_{j\alpha})^2}|RS\rangle}{\langle\Psi_T|RS\rangle} = \frac{\langle\Psi_T|\int \mathrm{d}y_2\mathrm{e}^{-\frac{y_2^2}{2}}\mathrm{e}^{\sqrt{\frac{\gamma}{2}}iy_2(\sigma_{i\gamma}\tau_{i\alpha}-\tau_{j\alpha})}|RS\rangle}{\langle\Psi_T|RS\rangle}. \tag{6.3}$$

Analytical result: $0.999\ 328\ 30(MeV)$

Monte Carlo result: $0.999\ 328\ 41(MeV)\pm 2.1\times10^{-7}(MeV)$

So the analytical result agrees with the Monte Carlo result.

(3) Results of the second auxiliary field y_1, y_2 with $\vec{x}_{ij\alpha}$ fixed. $\Delta t = 1 \times 10^{-6} MeV^{-1}$.

$$\begin{aligned} &\frac{\langle \Psi_T | e^{\gamma \sigma_{i\gamma} \tau_{i\alpha} \tau_{j\alpha}} | RS \rangle}{\langle \Psi_T | RS \rangle} \\ &= \frac{\langle \Psi_T | \int \mathrm{d}y_1 \mathrm{d}y_2 \mathrm{e}^{-\frac{y_1^2+y_2^2}{2}} \mathrm{e}^{\sqrt{\frac{\gamma}{2}}\{y_1(\sigma_{i\gamma}\tau_{i\alpha}+\tau_{j\alpha})+iy_2(\sigma_{i\gamma}\tau_{i\alpha}-\tau_{j\alpha})\}} | RS \rangle}{\langle \Psi_T | RS \rangle}. \end{aligned} \tag{6.4}$$

Analytical result: 0.998 655 40(MeV)

Monte Carlo result: 0.998 655 52$(MeV) \pm 2.7 \times 10^{-7}(MeV)$

So the analytical result agrees with the Monte Carlo result.

(4) Results of second auxiliary filed y_1, y_2, y_3, y_4 with $\vec{x}_{ij\alpha}$ fixed. $\Delta t = 1 \times 10^{-6}$.

$$\begin{aligned} &\frac{\langle \Psi_T | e^{\gamma(\sigma_{i\gamma}\tau_{i\alpha}\tau_{j\alpha}+\sigma_{j\gamma}\tau_{j\alpha}\tau_{i\alpha})} | RS \rangle}{\langle \Psi_T | RS \rangle} = \int \mathrm{d}y_1 \mathrm{d}y_2 \mathrm{d}y_3 \mathrm{d}y_4 \\ &\cdot \frac{\langle \Psi_T | \mathrm{e}^{-\frac{y_1^2+y_2^2+y_3^2+y_4^2}{2}} \mathrm{e}^{\sqrt{\frac{\gamma}{2}}\{y_1(\sigma_{i\gamma}\tau_{i\alpha}+\tau_{j\alpha})+iy_2(\sigma_{i\gamma}\tau_{i\alpha}-\tau_{j\alpha})+y_3(\sigma_{j\gamma}\tau_{j\alpha}+\tau_{i\alpha})+iy_4(\sigma_{j\gamma}\tau_{j\alpha}-\tau_{i\alpha})\}} | RS \rangle}{\langle \Psi_T | RS \rangle}. \end{aligned} \tag{6.5}$$

Analytical result: 0.998 305 40(MeV)

Monte Carlo result: 0.998 305 54$(MeV) \pm 6.8 \times 10^{-7}(MeV)$

So the analytical result agrees with the Monte Carlo result. Equation 6.5 has been checked.

Now we use the method in section 5.2 to check the whole spin-orbit-isospin propagator.

$$\begin{aligned} e^{-H_r \Delta t} = \prod_{\alpha, i<j} \frac{1}{(2\pi)^{\frac{3}{2}}} \int \mathrm{d}^3 x_{ij\alpha} \mathrm{e}^{-\frac{|x_{ij\alpha}|^2}{2}} \mathrm{e}^{\frac{3mA\Delta t}{32\hbar^2}[(\vec{\sigma}_i+\vec{\sigma}_j)\times\vec{r}_{ij}]^2[\frac{1}{3}v_{ls}(r_{ij})+\tau_{i\alpha}\tau_{j\alpha}v_{ls\tau}(r_{ij})]^2} \\ \cdot \mathrm{e}^{-\frac{i}{\hbar}\sqrt{\frac{4\Delta t\hbar^2}{3mA}}\left(\vec{p}_{ij}+\frac{3mA}{8\hbar}[(\vec{\sigma}_i+\vec{\sigma}_j)\times\vec{r}_{ij}][\frac{1}{3}v_{ls}(r_{ij})+\tau_{i\alpha}\tau_{j\alpha}v_{ls\tau}(r_{ij})]\right)\cdot\vec{x}_{ij\alpha}}. \end{aligned} \tag{6.6}$$

In order to make sure the propagator in equation 6.6 is correct, we separate the integrand into two pieces and calculate them separately for one time step. By setting

the momentum $\vec{p}_{ij}$ equal to zero, the mixed spin-orbit-isospin energy is calculated as:

$$\prod_{\alpha,i<j} \frac{1}{(2\pi)^{\frac{3}{2}}} \frac{\langle \Psi_T | \int \mathrm{d}^3 x_{ij\alpha} \mathrm{e}^{-\frac{|x_{ij\alpha}|^2}{2}} \mathrm{e}^{-\frac{i}{\hbar}\sqrt{\frac{3mA\Delta t}{16}}\left([(\vec{\sigma}_i+\vec{\sigma}_j)\times\vec{r}_{ij}][\frac{1}{3}v_{ls}(r_{ij})+\tau_{i\alpha}\tau_{j\alpha}v_{ls\tau}(r_{ij})]\right)\cdot\vec{x}_{ij\alpha}} | RS\rangle}{\langle \Psi_T | RS\rangle}. \tag{6.7}$$

It should have the same value of mixed energy of the counter term as in equation 6.6, but with opposite sign. The mixed energy of counter term is:

$$\frac{\langle \Psi_T | \mathrm{e}^{\frac{3mA\Delta t}{32\hbar^2}[(\vec{\sigma}_i+\vec{\sigma}_j)\times\vec{r}_{ij}]^2[\frac{1}{3}v_{ls}(r_{ij})+\tau_{i\alpha}\tau_{j\alpha}v_{ls\tau}(r_{ij})]^2} | RS\rangle}{\langle \Psi_T | RS\rangle} \tag{6.8}$$

The mixed energy of equations 6.7 and 6.8 are calculated and compared. They should agree within error bars. The two-nucleon results are listed, with $\rho = 0.48 fm^{-3}$, $\Delta t = 1 \times 10^{-6} MeV^{-1}$. In table 6.1, the mixed energy of propagator in 6.7 does

Table 6.1: Mixed Energy of Spin-Orbit-Isospin

mixed energy	mean value(MeV)	error bar(MeV)
propagator in 6.7	3.802	0.491
counter term in 6.8	-2.099	0.073
analytical result	2.089	

not agree with the mixed energy of the counter term in 6.8. We also calculated the analytical result of 6.7, which is $2.089(MeV)$. The result of counter term agrees with the analytical result, while the mixed energy of the spin-orbit-isospin term does not. In the following contents, we will show more investigation about $3.802(MeV)$ in table 6.1. So far, we have not found out any problems with the formula or algorithm. It could be round-off errors since the time step is very small, and we are trying to use time extrapolation to get reasonable results.

From the results of equations 6.2, 6.3, 6.4 and 6.5, we can see that the propagator with the second auxiliary field should be correct. Then the whole propagator in equation 6.6 needs to be checked. So we used Gaussian-Hermite sampling instead

of Monte Carlo sampling. The Gaussian-Hermite sampling points and weights are listed below. The results are converged. The result of Gaussian-Hermite calculation

Table 6.2: Gaussian-Hermite Sampling

sampling points	sampling weights
$-\sqrt{3.0-\sqrt{6.0}}$	$(3.0+\sqrt{6.0})/12.0$
$\sqrt{3.0-\sqrt{6.0}}$	$(3.0+\sqrt{6.0})/12.0$
$-\sqrt{3.0+\sqrt{6.0}}$	$(3.0-\sqrt{6.0})/12.0$
$\sqrt{3.0+\sqrt{6.0}}$	$(3.0-\sqrt{6.0})/12.0$

of equation 6.6 is $2.089(MeV)$, the same as the analytical result. Therefore the propagation in equation 6.6 should be correct. Since the propagation depends on the time step, we will plot how the mixed energy changes with the time step, and how the ratio $\frac{\langle\Psi_T|R'S'\rangle}{\langle\Psi_T|RS\rangle}$ changes with the time step. Figure 6.1 shows that the mixed spin-orbit-isospin energy changes a lot when time step changes. The ideal result of figure 6.1 should be a constant. Figure 6.2 shows that there are additional errors in the simulation of equation 6.6. We will check the variance in the next section.

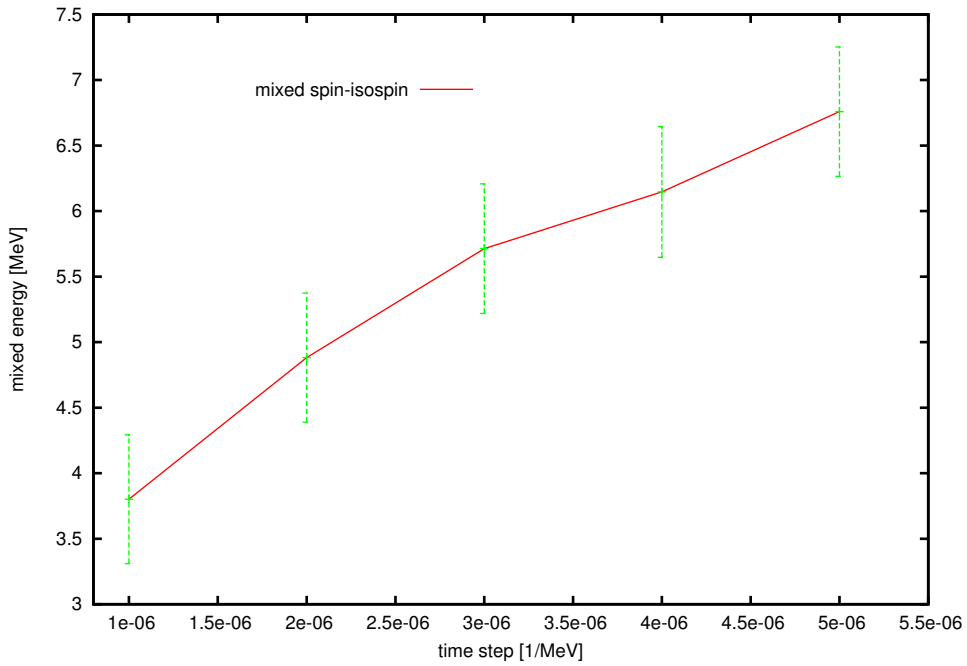

Figure 6.1: Mixed Energy of the Spin-Orbit-Isospin Interaction as Described in the Text.

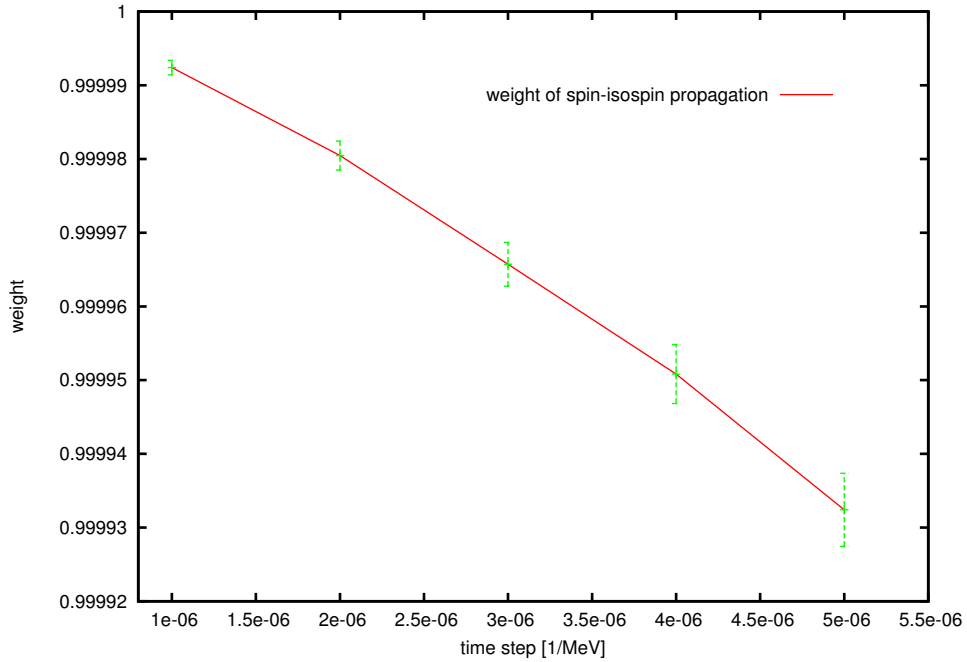

Figure 6.2: The Ratio of the Trial Wave Function vs. Time Step in the Spin-Orbit-Isospin Interaction as Described in the Text.

6.2 Checking the Variance

In last section, Figures 6.1 and 6.2 show that the statistical result of spin-orbit-isospin propagator is not as good as other potential operators in Argonne v8'. By using Gaussian-Hermite sampling, the result of equation 6.6 is the same as analytical result, so the equation 6.6 proved to be correct. This indicates that additional variance must be cancelled to obtain controlled variance in the Monte Carlo simulation. We need to check the variance in equation 6.6 to see if this is the problem.

From section 4.3, we know that mathematically, the variance could be eliminated by using the antithetic variables $\{\pm\vec{x}_{ij\alpha}, \pm\{y_1, y_2, y_3, y_4\}\}$. The checking of variance has been done in section 5.3 for the spin-orbit propagator. We will use the same method to check the variance for spin-orbit with isospin interaction.

Similarly, the ratio of one time-step propagation $\frac{\langle\Psi_T|R'S'\rangle}{\langle\Psi_T|RS\rangle}$ should be proportional to the time step Δt. We start from 1 walker, one component in equation 6.6, so there is no statistical error, and the ratio should be a linear line with time step.

Here we would like to show that the variables in 4.72 and 4.73 did eliminate the variance efficiently.

$$\{\{\pm\vec{x}_{ij\alpha}, \pm\{y_1, y_2, y_3, y_4\}\}, \{\pm\vec{x}_{ij\alpha}, \pm\{y_2, y_1, y_4, y_3\}\}\} \tag{6.9}$$

If we use the the variables in 4.70 and 4.71 $\{\pm\vec{x}_{ij\alpha}, \pm\{y_1, y_2, y_3, y_4\}\}$, the ratio in figure 6.3 would become that shown in figure 6.4.

We will henceforth use the 16 sets of variables of equation 6.9. It is good to see that in figure 6.3, the ratio of $\frac{\langle\Psi_T|R'S'\rangle}{\langle\Psi_T|RS\rangle}$ is a straight line. Figure 6.3 only checked the $\alpha = 1$ component in equation 6.6, that is, one component of $\tau_i \cdot \tau_j$ in spin-orbit-isospin interaction. Now we check the three components of $\tau_i \cdot \tau_j$ in equation 6.6 with 1 walker.

One thing needs to be noticed is that, when we expanded the propagator in

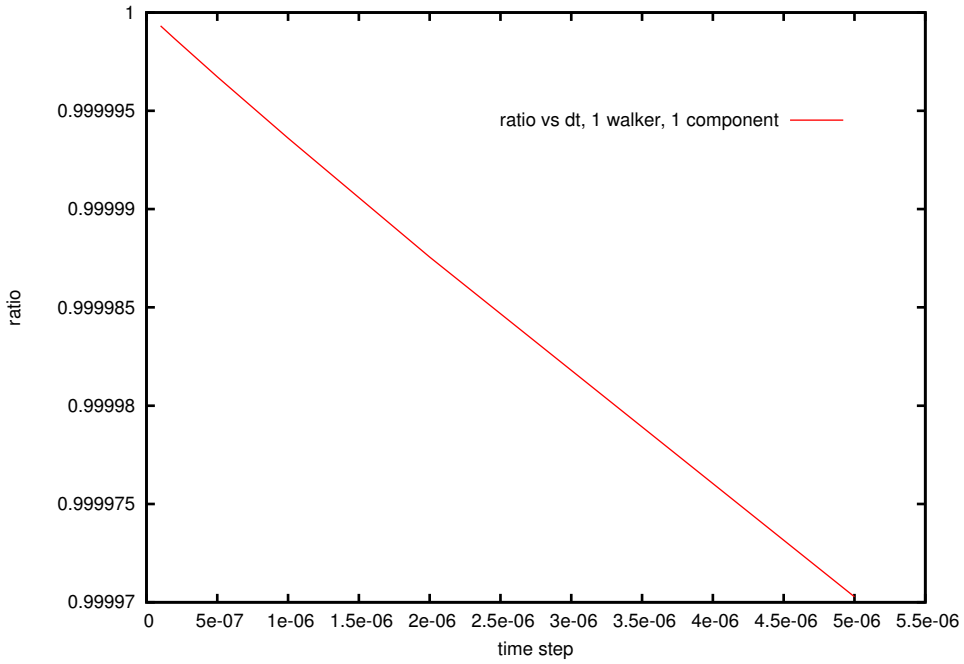

Figure 6.3: Same as Fig 6.2, Except Including Only 1 Component of the Propagator.

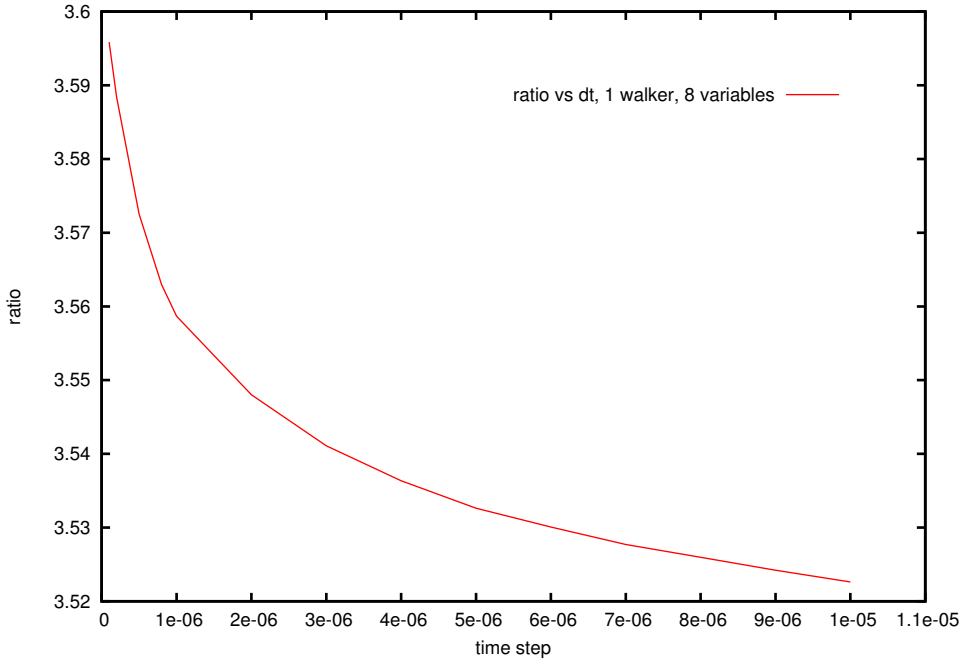

Figure 6.4: Same as Fig 6.3 But with 8 Antithetic Variables.

equation 4.63, there is variance at the order of $\sqrt{\Delta t}$ for the product of y_1 and y_2. y_1 and y_2 are independent Gaussian variables, so this kind of variance could happen between any other second auxiliary field variables. To avoid this problem, we calculate the ratio of the three components in equation 6.6 separately, then multiply them as the total ratio. The plot is in figure 6.5.

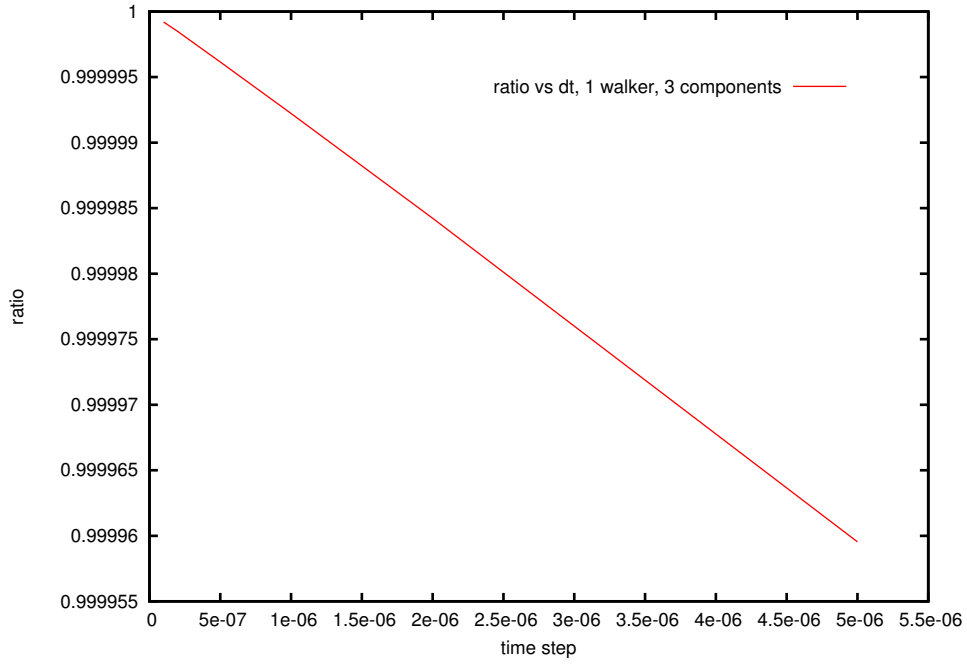

Figure 6.5: Same as Fig 6.2, 3 Components of Isospin.

We plot figures 6.3 and 6.5 together on one figure as figure 6.6. It shows that both of them are linear with time step; the difference is the slope. This makes sense; the mixed energy of one component of spin-orbit-isospin interaction should be different from the mixed energy of whole spin-orbit-isospin interaction.

The the mixed energy per 1 walker can be calculated. Because $|R'S'\rangle = e^{-H_r \Delta t}|RS\rangle$, and $\frac{\langle \Psi_T|R'S'\rangle}{\langle \Psi_T|RS\rangle}$ is known, so the mixed energy per particle corresponding to the known H_r is $-\frac{1}{\Delta t A}\langle \frac{\Psi_T(R'S')}{\Psi_T(RS)}\rangle (MeV)$. We calculate the mixed energies for the two cases, and plot the mixed energies against time step in figure 6.7

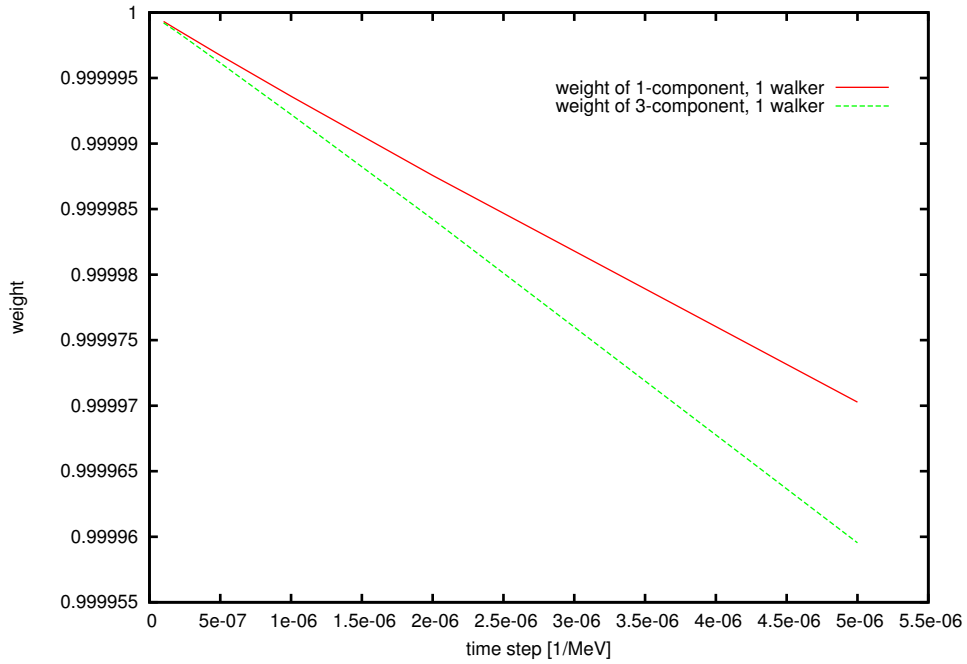

Figure 6.6: The Weight of the Trial Wave Function vs. Time Step in Spin-Orbit-Isospin Interaction of 1- and 3-Component.

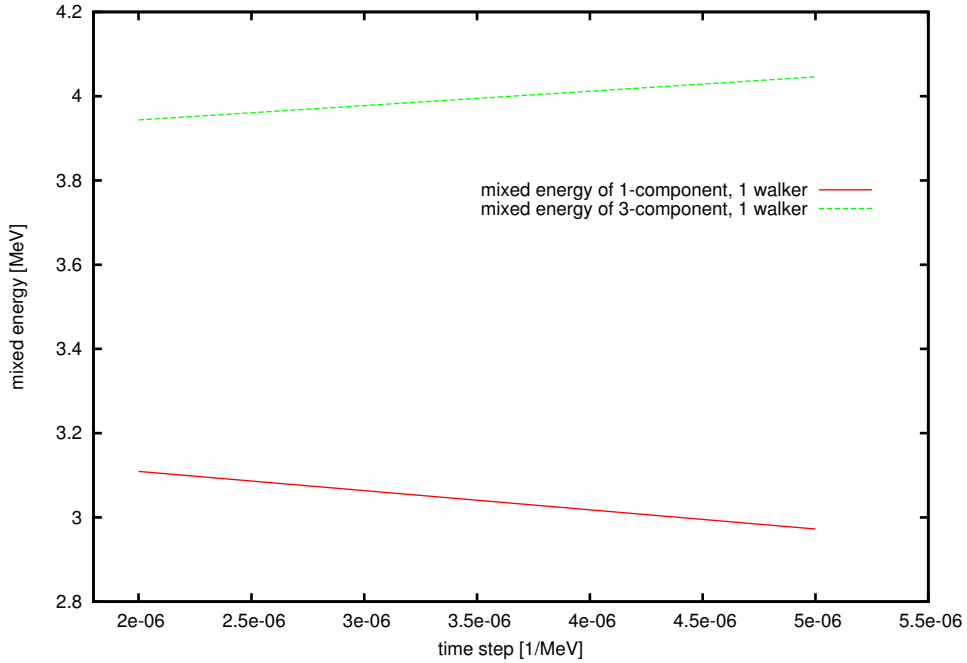

Figure 6.7: Mixed Energies of the Spin-Orbit-Isospin Interaction of 1- and 3-Component for 1 Walker.

The upper line in figure 6.7 is the mixed energy of $\vec{L}\cdot\vec{S}(\vec{\tau_i}\cdot\vec{\tau_j})$, while the lower line is the mixed energy of $\vec{L}\cdot\vec{S}(\tau_{i\alpha}\tau_{j\alpha})$. It is reasonable that the former one is higher than the latter one. Both the two mixed energies should be constant in an ideal situation. But in figure 6.7, they both show changes with the time step, indicating time step errors. The behavior at small Δt is from round-off error. Because they are directly calculated from figure 6.6, there is no variance in figure 6.6, so the non-constant is not caused by variance. Also, we only use one walker for the calculation, so there is no statistical error either. Since the time step is very small, round-off error is possible.

Then we need to use more walkers to sample the mixed energies in figure 6.7. The mean values of sampled results are plotted against time step in figure 6.8. The lower line is the sampled mixed energy for one component in spin-orbit-isospin. It behaves as a constant value in figure 6.8, which is expected. The upper line is the sampled mixed energy for the whole spin-orbit-isospin. It changes a lot with the time step, which is the same problem in figure 6.1, where the mixed energy of sampled propagator does not agree with analytical result for $\Delta t = 1 \times 10^{-6} MeV^{-1}$ in table 6.1.

To investigate the problem, we separated the operators in equation 6.6, and checked the one-step propagation for one walker. We did not find anything wrong with the formula or algorithm for one walker. Though there might be round-off errors in figure 6.7, which could be the reason causing the problem in figure 6.8. This problem is not yet solved. Meanwhile, we will calculate the ground-state energy in the same way as chapter 5 with the full Argonne v8'.

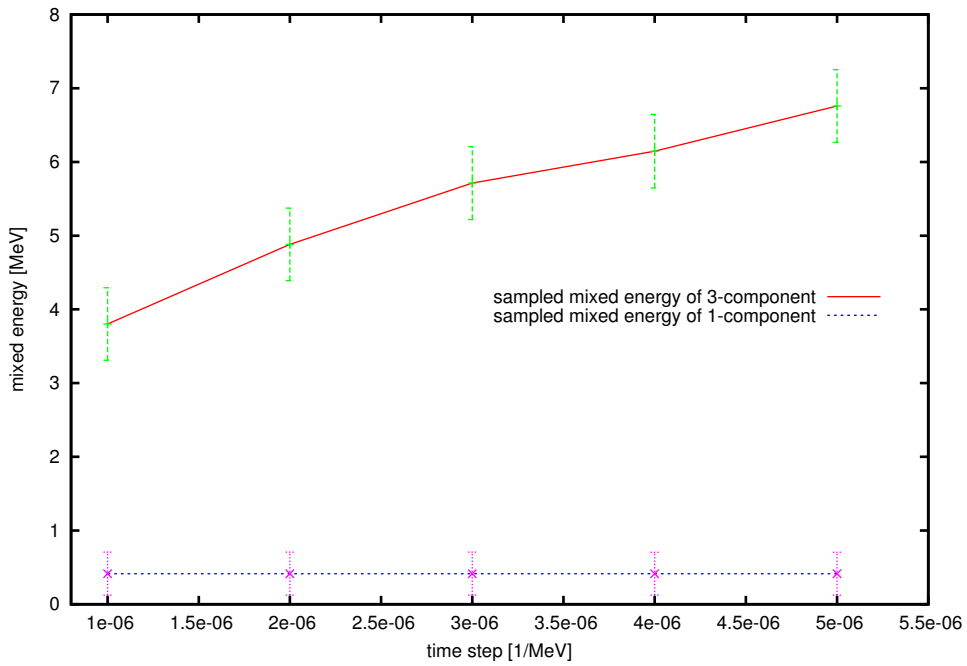

Figure 6.8: Sampled Mixed Energies of the Spin-Orbit-Isospin Interaction of 1- and 3-Component.

6.3 Results of Spin-Orbit with Isospin

The problem of the mixed energy for the calculation of $\vec{L}\cdot\vec{S}(\vec{\tau}_i\cdot\vec{\tau}_j)$ in last section could be caused by round-off errors. This requires additional research. In this section, we will calculate the diffusion results for a two-nucleon system.

As introduced in chapter 3, we use $e^{i\vec{k}\cdot\vec{r}}$ for the space part of the orbitals for the many-body trial wave functions. The momentum $\vec{k}$ is zero for two nucleons in their ground state. In order to have a spin-orbit interaction for two nucleons, we set the momentum in the orbitals to be as

$$\vec{k}_1 = (0,0,0)\,, \qquad \vec{k}_2 = (1,0,0)\,. \tag{6.10}$$

So the ground-state energy would be positive for the two-nucleon system in this case. The ground-state energy of Argonne v8' has been calculated and listed in table 6.3. We also calculated the ground-state energy without spin-orbit interactions, written

as v6, and the one including the spin-orbit without isospin interaction, written as v7 in the table. The column v8 refers to the full Argonne v8'. The time step is $\Delta t = 1 \times 10^{-6} MeV^{-1}$.

Table 6.3: Ground-State Energy for A=2

	mean value (MeV)	error (MeV)
v6	164.47	0.46
v7	160.21	0.74
v8	168.27	0.97

In table 6.3, the results of 'v6' and 'v7' look reasonable, because the spin-orbit interactions are attractive forces, which will decrease the ground state energy. The result including spin-orbit with isospin is much greater than the other two. So we explored the time-step dependence of the energy. The time step is decreased to $1 \times 10^{-7} MeV^{-1}$. The results are plotted with error bars. In figure 6.9, the ground-

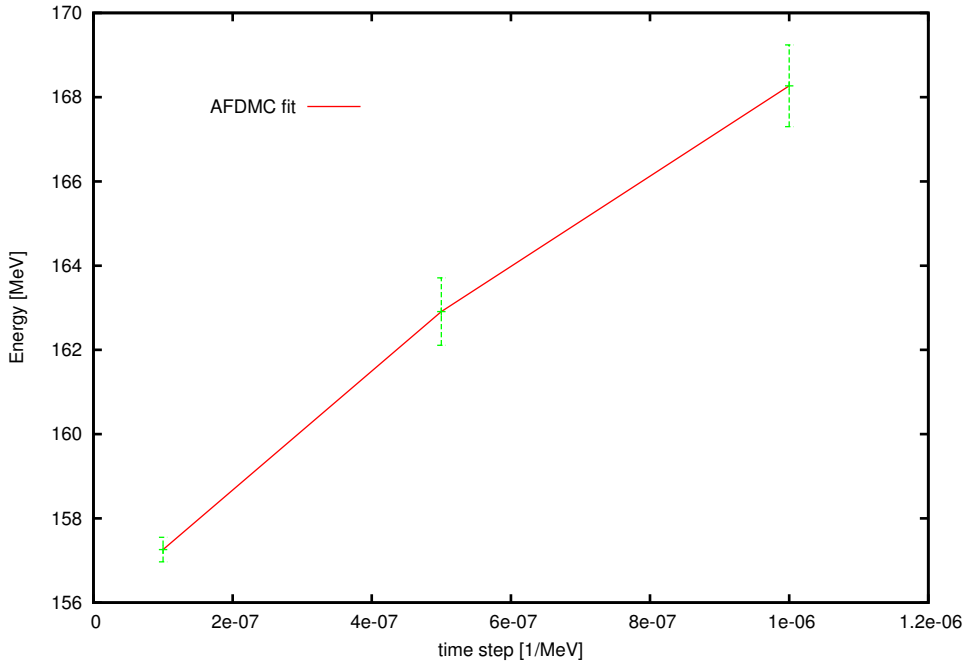

Figure 6.9: Ground-State Energy with v8'.

state energy decreases when the time step is smaller. The large time step error must be extrapolated out to get accurate results. The Lanczos method in Appendix A can be employed to check the local energy for the two-nucleon system in periodic boundary conditions.

6.4 Future Plan

The future plan of this work is to make sure the spin-orbit interactions in auxiliary field Monte Carlo agrees with the Lanczos method for the two-nucleon system. Then we can apply the method to the 28 nucleon system, and calculate the equation of state in nuclear matter with the full Argonne v8'.

Once the Argonne v8' is simulated, the three-body potential introduced in chapter 2 could be added in the Hamiltonian.

Chapter 7

CONCLUSION

The spin-orbit interactions are important to include to investigate nuclear structures. They are difficult to calculate in auxiliary field diffusion Monte Carlo, since the product of three operators will increase the scaling exponentially. In this work, we employed the Hubbard-Stratonovich transformation twice to break up the interactions between two nucleons, so the spin-orbit interactions can be calculated for the Argonne v8' potential.

Pair-wise propagation has been developed in this work to calculate the spin-orbit interactions. To calculate the $\vec{L}\cdot\vec{S}$ and $\vec{L}\cdot\vec{S}(\vec{\tau}_i\cdot\vec{\tau}_j)$, we combined these two terms with the kinetic energy as H_r, and used the first auxiliary field to linearize the operators in H_r. Since the operators in H_r operate on pairs of nucleons independently, we developed pair-wise propagation for the propagator with H_r, and diffused the walkers to the new states with the weight of local energy. The pair-wise propagation is equivalent to the previous single-particle propagation for the kinetic energy parts, because they give the same distributions only sampled differently. We checked the pair-wise propagation by comparing the results of pair-wise propagation and single-particle propagation for different Hamiltonians. For each Hamiltonian, the results of the two propagations agreed within error bars. Therefore, the pair-wise propagation has been checked correctly and could be used to calculate the spin-orbit interactions.

We also developed the method of antithetic variables in this work to eliminate the variance in the second auxiliary field. Previous AFDMC used shifted Gaussian variables to calculate the Hamiltonian with Argonne v6'. Since there was only the first auxiliary field in the calculation, the shifted Gaussian variables worked well in the

truncated propagators with error terms of order Δt^2. However, when we calculated the Hamiltonian with Argonne v8' which includes the spin-orbit interactions, a second auxiliary field was necessary to be employed, where the shifted Gaussian variables caused variances which have the lower order than Δt. To eliminate these variances, we developed the antithetic variables to cancel the non-zero terms in the sums of the second auxiliary field. By plotting the weight of one time-step propagation against time step, we can show that the variances in the second auxiliary field have been eliminated thoroughly by using the antithetic variables.

The spin-orbit without isospin interaction was calculated successfully in this work. By combining this interaction with the kinetic energy, and using the antithetic variables, we calculated the ground state energies of symmetric nuclear matter in different densities, and plotted the equation of state of symmetric nuclear matter. From the figure 5.3 we can see that the spin-orbit without isospin interaction decreased the ground state energies of the Hamiltonian with Argonne v6' as expected, because spin-orbit interactions are attractive forces. The decreased energy has been checked by calculating the one time-step propagation differently, and proved to be correct.

With the inclusion of the isospin-dependent spin-orbit interaction, we can apply the method to neutron-rich nuclei and see how the spin-orbit interaction changes the energy levels in nuclei.

REFERENCES

[1] Henning Heiselberg and Vijay Pandharipande. Recent progresses in neutron star theory. *Annu. Rev. Nucl. Part. Sci.*, 50:481, 2000.

[2] J. M. Lattimer and M. Prakash. Neutron star structure and the equation of state. *Astrophys. J.*, 550:426, 2001.

[3] J. M. Lattimer and M. Prakash. The physics of neutron stars. *Science*, 304:536, 2004.

[4] W.S.C. Williams. *Nuclear and particle physics*. oxford science publications, 1991.

[5] J. D. Walecka. *Theoretical nuclear and subnuclear physics*. world scientific, 1995.

[6] P.D. Cottle and K.W. Kemper. A walk along the dripline.

[7] R. Lacey P. Danielewicz and W. G. Lynch. Determination of the equation of state of dense matter. *Science*, 298:1592, 2002.

[8] O. Y. Gnedin D.G. Yakovlev, A. D. Kaminker and P. Haensel. Neutrino emission from neutron stars. *Phys. Rep*, 354:1, 2001.

[9] Gerald E. Brown and T.T.S. Kuo. *The Nucleon-nucleon Interaction and the Nuclear Many-body Problem*. World Scientific, 2010.

[10] D. G. Ravenhall C. P. Lorenz and C. J. Pethick. Neutron star crusts. *Phys. Rev. Lett.*, 70:379382, 1993.

[11] David J. Dean. Beyond the nuclear shell model. *Physics today*, 60:48, 2007.

[12] K. Orginos S.R. Beane, W. Detmold and M.J. Savage. Nuclear physics from lattice qcd. *Progress in Particle and Nuclear Physics*, 66:1, 2011.

[13] W. Gl ckle and H. Kamada. Alpha-particle binding energies for realistic nucleon-nucleon interactions. *Phys. Rev. Lett.*, 71:971974, 1993.

[14] N. Barnea W. Leidemann S. Bacca, M.A. Marchisio and G. Orlandini. Microscopic calculation of six-body inelastic reactions with complete final state interaction: Photoabsorption of 6 he and 6 li. *Phys. Rev. Lett.*, 89:052502, 2002.

[15] W. Leidemann S. Bacca, N. Barnea and G. Orlandini. Effect of p-wave interaction in 6 he and 6 li photoabsorption. *Phys. Rev. C*, 69:057001, 2004.

[16] J. P. Vary W. E. Ormand P. Navr til, V. G. Gueorguiev and A. Nogga. Structure of a = 10 13 nuclei with two- plus three-nucleon interactions from chiral effective field theory. *Phys. Rev. Lett.*, 99:042501, 2007.

[17] R. Roth and P. Navr til. Ab initio study of 40 ca with an importance truncated no-core shell model. *Phys. Rev. Lett.*, 99:092501, 2007.

[18] M. Hjorth-Jensen T. Papenbrock D.J. Dean, G. Hagen and A. Schwenk. Comment on ab initio study of 40 ca with an importance-truncated no-core shell model. *arXiv:0709.0449 [nucl-th]*, 2007.

[19] R. B. Wiringa. Variational calculations of few-body nuclei. *Phys. Rev. C*, 43:15851598, 1991.

[20] R.B. Wiringa. Monte carlo calculations of few-body and light nuclei. *Nucl. Phys. A*, 543:199c, 1992.

[21] J. Carlson. Greens function monte carlo study of light nuclei. *Phys. Rev. C*, 36:2026–2033, 1987.

[22] J.Carlson B.S. Pudliner, V.R. Pandharipande and R.B. Wiringa. Quantum monte carlo calculations of a 6 nuclei. *Phys. Rev. Lett.*, 74:4396–4399, 1995.

[23] V.R. Pandharipande J. Carlson, J. Morales and D.G. Ravenhall. Quantum monte carlo calculations of neutron matter. *Phys. Rev. C*, 68:025802, 2003.

[24] J. Carlson. Gfmc studies of low-density neutron matter. *Eur. Phys. J. A*, 17:463, 2003.

[25] Jr.-V. R. Pandharipande D. G. Ravenhall J. Carlson Steven C. Pieper R. B. Wiringa S. Y. Chang, J. Morales and K. E. Schmidt. Neutron matter: A superfluid gas. *Nucl. Phys. A*, 746:215, 2004.

[26] Steven C. Pieper. Quantum monte carlo calculations of light nuclei. *Nucl. Phys. A*, 751:516, 2005.

[27] K.E. Schmidt and S. Fantoni. A quantum monte carlo method for nucleon systems. *Phys. Lett. B*, 446:99, 1999.

[28] A. Sarsa S. Fantoni and K.E. Schmidt. A new quantum monte carlo method for nucleon systems. *Prog. Part. Nucl. Phys.*, 44:65, 2000.

[29] A. Sarsa S. Fantoni and K.E. Schmidt. Spin susceptibility of neutron matter at zero temperature. *Phys. Rev. Lett.*, 87:181101, 2001.

[30] S. Fantoni S. Gandolfi, F. Pederiva and K.E. Schmidt. Quantum monte carlo calculations of symmetric nuclear matter. *Phys. Rev. Lett.*, 98:102503, 2007.

[31] J. Hope. Nuclear spin-orbit energy for oscillator wave functions. *Phys. Rev.*, 106:771, 1957.

[32] N. Kaiser. Nuclear spinorbit interaction from chiral pionnucleon dynamics. *Nucl. Phys. A*, 709:251274, 2002.

[33] A. Polls I. Bombaci, A. Fabrocini and I. Vidana. Spin-orbit and tensor interactions in homogeneous matter of nucleons: accuracy of modern many-body theories. *Phys. Lett. B*, 609:232–240, 2005.

[34] John J. Rusnak R.J. Furnstahl and Brian D. Serot. The nuclear spin-orbit force in chiral effective field theories. *Nucl. Phys. A*, 632:607–623, 1998.

[35] T. Gajewski. Polarization by spin-orbit forces in nucleon-nucleon scattering. *Nuclear physics*, 41:328–329, 1963.

[36] V. R. Pandharipande A. Akmal and D. G. Ravenhall. Equation of state of nucleon matter and neutron star structure. *Phys. Rev. C*, 58:1804, 1998.

[37] R.B. Wiringa and Steven C. Pieper. Evolution of nuclear spectra with nuclear forces. *Phys. Rev. Lett.*, 89:182501, 2002.

[38] W. Gloeckle E. Epelbaum and Ulf-G. Meissner. The two-nucleon system at next-to-next-to-next-to-leading order. *Nucl. Phys. A*, 747:362, 2005.

[39] D.R. Entem and R. Machleidt. Accurate charge-dependent nucleon-nucleon potential at fourth order of chiral perturbation theory. *Phys. Rev. C*, 68:041001, 2003.

[40] T.S.H. Lee M. Betz. Phenomenological hamiltonian for pions, nucleons, and δ isobars: Application to the pion-deuteron system. *Phys. Rev. C*, 23:1, 1981.

[41] Stefano Gandolfi. The equation of state of neutron matter, symmetry energy, and neutron star structure. *J. Phys*, 420:012150, 2013.

[42] R.A. Smith R.B. Wiringa and T.L. Ainsworth. Nucleon-nucleon potentials with and without (1232) degrees of freedom. *Phys. Rev. C*, 29:1207, 1984.

[43] I. E. Lagaris and V. R. Pandharipande. Phenomenological two-nucleon interaction operator. *Nucl. Phys. A*, 359:331348, 1981.

[44] K. Holinde R. Machleidt and Ch. Elster. The bonn meson-exchange model for the nucleonnucleon interaction. *Phys. Rep.*, 149:1, 1987.

[45] R. Machleidt. Nuclear forces and nuclear structure. *Adv. Nucl. Phys.*, 19:189, 1989.

[46] J.M. Richard-R. Vinh Mau J. Cote P. Pires M. Lacombe, B. Loiseau and R. de Tourreil. Parametrization of the paris nn potential. *Phys. Rev. C*, 21:861, 1980.

[47] Jr. R.V. Reid. Local phenomenological nucleon-nucleon potentials. *Ann. Phys. (N.Y.)*, 50:411, 1968.

[48] M. C. M. Rentmeester V. G. J. Stoks, R. A. M. Klomp and J. J. de Swart. Partial-wave analysis of all nucleon-nucleon scattering data below 350 mev. *Phys. Rev. C*, 48:792–815, 1993.

[49] T.A. Rijken M.M. Nagels and J.J. de Swart. Low-energy nucleon-nucleon potential from regge-pole theory. *Phy. Rev. D*, 17:768, 1978.

[50] C. P. F. Terheggen V. G. J. Stoks, R. A. M. Klomp and J. J. de Swart. Construction of high-quality nn potential models. *Phys. Rev. C*, 49:2950–2962, 1994.

[51] V. G. J. Stoks R. B. Wiringa and R. Schiavilla. Accurate nucleon-nucleon potential with charge-independence breaking. *Phys. Rev. C*, 51:3851, 1995.

[52] K. Varga Steven C. Pieper and R. B. Wiringa. Quantum monte carlo calculations of a = 9, 10 nuclei. *Phys. Rev. C*, 66:044310, 2002.

[53] J. Carlson R. B. Wiringa, Steven C. Pieper and V. R. Pandharipande. Quantum monte carlo calculations of a = 8 nuclei. *Phys. Rev. C*, 62:014001, 2000.

[54] J. Carlson Steven C. Pieper B.S. Pudliner, V.R. Pandharipande and R.B. Wiringa. Quantum monte carlo calculations of nuclei with a 7. *Phys. Rev. C*, 56:1720–1750, 1997.

[55] Rob Timmermans Vincent Stoks and J. J. de Swart. Pion-nucleon coupling constant. *Phys. Rev. C*, 47:512520, 1993.

[56] R. B. Wiringa Steven C. Pieper and J. Carlson. Quantum monte carlo calculations of excited states in a = 6 8 nuclei. *Phys. Rev. C*, 70:054325, 2004.

[57] V. R. Pandharipande A. Akmal and D. G. Ravenhall. Equation of state of nucleon matter and neutron star structure. *Phys. Rev. C*, 58:18041828, 1998.

[58] Robert B. Wiringa. Interplay between two- and three-body interaction in light nuclei and nuclear matter. *Nucl. Phys. A*, 401:86, 1983.

[59] Sidney A. Coon and Walter Glckle. Two-pion-exchange three-nucleon potential: Partial wave analysis in momentum space. *Phys. Rev. C*, 23:1790–1802, 1981.

[60] R. A. Smith R. B. Wiringa and T. L. Ainsworth. Nucleon-nucleon potentials with and without (1232) degrees of freedom. *Phys. Rev. C*, 29:1207–1221, 1984.

[61] R. B. Wiringa Steven C. Pieper, V. R. Pandharipande and J. Carlson. Realistic models of pion-exchange three-nucleon interactions. *Phys. Rev. C*, 64:014001, 2001.

[62] R. A. Rice A. Picklesimer and R. Brandenburg. Trinuclear components and the triton binding energy. *Phys. Rev. Lett.*, 68:1484–1487, 1992.

[63] R. A. Rice A. Picklesimer and R. Brandenburg. degrees of freedom in trinuclei: I. the hannover one- model. *Phys. Rev. C*, 44:1359–1379, 1991.

[64] R. A. Rice A. Picklesimer and R. Brandenburg. degrees of freedom in trinuclei. ii. the hannover model. *Phys. Rev. C*, 45:547–562, 1992.

[65] R. A. Rice A. Picklesimer and R. Brandenburg. degrees of freedom in trinuclei. iii. the argonne model. *Phys. Rev. C*, 45:2045–2054, 1992.

[66] R. A. Rice A. Picklesimer and R. Brandenburg. degrees of freedom in trinuclei. iv. effects. *Phys. Rev. C*, 45:2624–2627, 1992.

[67] R. A. Rice A. Picklesimer and R. Brandenburg. degrees of freedom in trinuclei. v. exotic contributions. *Phys. Rev. C*, 46:1178–1182, 1992.

[68] V. R. Pandharipande J. Carlson and R. B. Wiringa. Three-nucleon interaction in 3-, 4- and -body systems. *Nucl. Phys. A*, 401:59, 1983.

[69] Steven Weinberg. Nuclear forces from chiral lagrangians. *Physics Letters B*, 251:288292, 1990.

[70] Dean Lee Evgeny Epelbaum, Hermann Krebs and Ulf-G. Meiner. Ab initio calculation of the hoyle state. *Phys. Rev. Lett*, 106:192501, 2011.

[71] M. H. Kalos. Monte carlo calculations of the ground state of three- and four-body nuclei. *Phys. Rev.*, 128:17911795, 1962.

[72] M. Viviani. Few- and many-body methods in nuclear physics. *Eur. Phys. J. A.*, 31:429, 2007.

[73] James B. Anderson. A random-walk simulation of the schrodinger equation:h˙3ˆ+. *J. Chem. Phys.*, 63:1499, 1975.

[74] D. M. Ceperley and B. J. Alder. Ground state of the electron gas by a stochastic method. *Phys. Rev. Lett.*, 45:566–569, 1980.

[75] Lubos Mitas. Quantum monte carlo methods in physics and chemistry. *NATO Advanced Study Institute on QMC*, pages ed. by M. P. Nightingale and C. J. Umrigar, Cornell, 1999.

[76] Hagen. Kleinert. Hubbard-stratonovich transformation: Successes, failure, and cure. *Electron.J.Theor.Phys.*, 8:57, 2011.

[77] S. T. Tokdar and R. E. Kass. Importance sampling: A review. *WIREs Comp. Stat.*, 2:54–60, 2010.

[78] Shiwei Zhang and Henry Krakauer. Quantum monte carlo method using phase-free random walks with slater determinants. *Phys. Rev. Lett.*, 90:136401, 2003.

[79] J. Carlson Shiwei Zhang and J. E. Gubernatis. Constrained path quantum monte carlo method for fermion ground states. *Phys. Rev. Lett.*, 74:3652–3655, 1995.

[80] J. Carlson Shiwei Zhang and J. E. Gubernatis. Constrained path monte carlo method for fermion ground states. *Phys. Rev. B*, 55:7464–7477, 1997.

[81] J. Piekarewicz. Unmasking the nuclear matter equation of state. *Phys. Rev. C*, 69:041301, 2004.

[82] V. R. Pandharipande and R. B. Wiringa. Variations on a theme of nuclear matter. *Rev. Mod. Phys.*, 51:821861, 1979.

[83] A. Polls I. Bombaci, A. Fabrocini and I. Vidana. Spin-orbit tensor interactions in homogeneous matter of nucleons: accurancy of modern many-body theories. *Phys. Lett. B*, 609:232, 2005.

[84] S. Fantoni K.E. Schmidt and A. Sarsa. Constrained path calculations of the 4he and 16o nuclei. *Eur. Phys. J. A*, 17:469, 2003.

[85] B.G. Todd and J. Piekarewicz. Relativistic mean-field study of neutron-rich nuclei. *Phys. Rev. C*, 67:044317, 2003.

[86] Bao-An Li. Probing the high density behavior of the nuclear symmetry energy with high energy heavy-ion collisions. *Phys. Rev. Lett.*, 88:192701, 2002.

[87] R. F. Bishop J.C. Owen and J.M. Irvine. Model nuclear matter calculations with a new fermion lowest order constrained variational method. *Nucl. Phys. A*, 274:108, 1976.

[88] J.M. Irvine C. Howes and R.F. Bishop. Constrained variational results for the new bethe homework problem. *J. Phys. G: Nucl. Phys.*, 4:L45, 1978.

[89] V. R. Pandharipande J. Carlson and R. B. Wiringa. Three-nucleon interaction in 3-, 4- and -body systems. *Nucl. Phys. A*, 401:59, 1983.

[90] M. Baldo and C. Maieron. Spin-orbit correlation energy in neutron matter. *Phys. Rev. C*, 69:014301, 2004.

[91] A.Sarsa K.E.Schmidt L.Brualla, S.Fantoni and S.A.Vitiello. Spin-orbit induced backflow in neutron matter with auxiliary field diffusion monte carlo method. *Phys. Rev. C*, 67:065806, 2003.

[92] V. R. Pandharipande J. Carlson, J. Morales and D. G. Ravenhall. Quantum monte carlo calculations of neutron matter. *Phys. Rev. C*, 68:025802, 2003.

[93] S. Fantoni and K.E. Schmidt. Fermi hypernetted chain calculations in a periodic box. *Nuclear Physics A*, 690:456–470, 2001.

[94] J. Carlson V. R. Pandharipande Steven C. Pieper B. S. Pudliner, A. Smerzi and D. G. Ravenhall. Neutron drops and skyrme energy-density functionals. *Phys. Rev. Lett.*, 76:2416–2419, 1996.

[95] D. G. Ravenhall A. Smerzi and V. R. Pandharipande. Neutron drops and neutron pairing energy. *Phys. Rev. C*, 56:2549–2556, 1997.

[96] K. E. Schmidt F. Pederiva, A. Sarsa and S. Fantoni. Auxiliary field diffusion monte carlo calculation of ground state properties of neutron drops. *Nucl. Phys. A*, 742:255–268, 2004.

[97] J. Carlson Kevin E. Schmidt S. Gandolfi, A. Lovato. From the lightest nuclei to the equation of state of asymmetric nuclear matter with realistic nuclear interactions. *arXiv:1406.3388 [nucl-th]*, 2014.

APPENDIX A

LANCZOS MODEL

The spin-orbit with isospin $\vec{L} \cdot \vec{S}(\vec{\tau}_i \cdot \vec{\tau}_j)$ in Argonne v8' has never been calculated in nuclear matter. This work is to use auxiliary field to simulate these interactions. In order to make sure the calculations are correct, we will use the Lanczos model to double-check the spin-orbit interactions.

The Lanczos model shares Hamiltonian and periodic boundary conditions with auxiliary field Monte Carlo. We chose a full basis for two-nucleon wave functions, so the simulation is the exact integral of Schroedinger equations. The Lanczos algorithm has been checked by calculating the binding energy of the deuteron. The binding energy of the deuteron in our simulation is 2.2 MeV, agreeing with the experimental result. So the mathematics and algorithms of Lanczos model should be correct. Once we have the result of spin-orbit interactions in auxiliary field Monte Carlo, we could compare it with the one by using Lanczos. Now we will give a detailed introduction to the Lanczos model.

The full basis of the wave function in two nucleons is as follows.

$$\begin{aligned}
&F_{sss}|\uparrow\uparrow\rangle, \\
&F_{sss}|\downarrow\downarrow\rangle, \\
&iG_{aas}|\downarrow\downarrow\rangle, \\
&\frac{1}{\sqrt{2}}F_{asa}|\uparrow\downarrow + \downarrow\uparrow\rangle, \\
&\frac{1}{\sqrt{2}}iG_{saa}|\uparrow\downarrow + \downarrow\uparrow\rangle, \\
&iG_{aas}|\uparrow\uparrow\rangle.
\end{aligned} \tag{A.1}$$

The six basis elements are composed of two parts: positions and spinors. The position part is written as F or G, where F refers to the real part of the wave function, G refers to the imaginary part of the wave function. The subscript s and a refer to symmetric and antisymmetric. Since the boundary condition is periodic, the coordinates used are Cartesian coordinates. For each function, there are three subscripts for the three

components of the Cartesian coordinates. Take $iG_{aas}|\downarrow\downarrow\rangle$ for example. This basis is the imaginary part, in which the wave function is antisymmetric in the x component, antisymmetric in the y component, symmetric in the z component. The spinor part is spin-down for both nucleons. We only have a spin part for the two-nucleon system because the isopin in the deuteron is in the singlet state with value -3, while the spin in the deuteron is in triplet states with value 1.

Now we calculate the Hamiltonian matrix with the basis A.1. Since the basis is full basis in Cartesian space, we could use a Fourier transformation to calculate the kinetic energy. For the potential energy, the Argoone v8' in the deuteron has:

$$\begin{aligned}
1 &\longrightarrow 1,\\
\vec{\tau}_i\cdot\vec{\tau}_j &\longrightarrow -3,\\
\vec{\sigma}_i\cdot\vec{\sigma}_j &\longrightarrow 1,\\
(\vec{\tau}_i\cdot\vec{\tau}_j)(\vec{\sigma}_i\cdot\vec{\sigma}_j) &\longrightarrow -3,\\
\vec{S} &\longrightarrow 3\vec{\sigma}_i\cdot\hat{r}_{ij}\vec{\sigma}_j\cdot\hat{r}_{ij}-1,\\
\vec{S}(\vec{\tau}_i\cdot\vec{\tau}_j) &\longrightarrow -9\vec{\sigma}_i\cdot\hat{r}_{ij}\vec{\sigma}_j\cdot\hat{r}_{ij}+3,\\
\vec{L}\cdot\vec{S} &\longrightarrow \vec{L}\cdot\vec{S},\\
\vec{L}\cdot\vec{S}(\vec{\tau}_i\cdot\vec{\tau}_j) &\longrightarrow -3\vec{L}\cdot\vec{S}.
\end{aligned} \tag{A.2}$$

The first six operators in A.2 do not need Fourier transformation, and only tensor operators rotate the spinor. So we calculate these six operators first. In Cartesian coordinates, we have:

$$\vec{\sigma}_i\cdot\hat{r}_{ij}\vec{\sigma}_j\cdot\hat{r}_{ij}=(\sigma_{ix}\frac{x}{r}+\sigma_{iy}\frac{y}{r}+\sigma_{iz}\frac{z}{r})(\sigma_{jx}\frac{x}{r}+\sigma_{jy}\frac{y}{r}+\sigma_{jz}\frac{z}{r}). \tag{A.3}$$

Take the operator $\sigma_{ix}\sigma_{jx}\frac{x^2}{r^2}$ and basis $iG_{aas}|\downarrow\downarrow\rangle$ for example. The $\sigma_{ix}\sigma_{jx}$ will rotate the $|\downarrow\downarrow\rangle$ to $|\uparrow\uparrow\rangle$, and the $\frac{x^2}{r^2}$ does not change the symmetry of the wave function, so $iG_{aas}|\downarrow\downarrow\rangle$ becomes $iG_{aas}|\uparrow\uparrow\rangle$ with coefficient $\frac{x^2}{r^2}$. The matrix of the first six operators in A.2 is as follows, with basis A.1.

$$\begin{pmatrix} \frac{z^2}{r^2} & \frac{x^2-y^2}{r^2} & \frac{2xy}{r^2} & \frac{\sqrt{2}xz}{r^2} & \frac{\sqrt{2}yz}{r^2} & 0 \\ \frac{x^2-y^2}{r^2} & \frac{z^2}{r^2} & 0 & -\frac{\sqrt{2}xz}{r^2} & \frac{\sqrt{2}yz}{r^2} & -\frac{2xy}{r^2} \\ \frac{2xy}{r^2} & 0 & \frac{z^2}{r^2} & -\frac{\sqrt{2}yz}{r^2} & -\frac{\sqrt{2}xz}{r^2} & \frac{x^2-y^2}{r^2} \\ \frac{\sqrt{2}xz}{r^2} & -\frac{\sqrt{2}xz}{r^2} & -\frac{\sqrt{2}yz}{r^2} & \frac{x^2+y^2-z^2}{r^2} & 0 & -\frac{\sqrt{2}yz}{r^2} \\ \frac{\sqrt{yz}}{r^2} & \frac{\sqrt{yz}}{r^2} & -\frac{\sqrt{xz}}{r^2} & 0 & \frac{x^2+y^2-z^2}{r^2} & \frac{\sqrt{xz}}{r^2} \\ 0 & -\frac{2xy}{r^2} & \frac{x^2-y^2}{r^2} & -\frac{\sqrt{2}yz}{r^2} & \frac{\sqrt{2}xz}{r^2} & \frac{z^2}{r^2} \end{pmatrix}. \tag{A.4}$$

Then we calculate the $\vec{L} \cdot \vec{S}$ terms.

$$\begin{aligned} \vec{L} \cdot \vec{S} &= \frac{1}{2\hbar} \vec{p}_{ij} \cdot [(\vec{\sigma}_i + \vec{\sigma}_j) \times \vec{r}_{ij}] \\ &= -i\hbar\nabla_x [z(\sigma_{iy} + \sigma_{jy}) - y(\sigma_{iz} + \sigma_{jz})] \\ &\quad - i\hbar\nabla_y [x(\sigma_{iz} + \sigma_{jz}) - z(\sigma_{ix} + \sigma_{jx})] \\ &\quad - i\hbar\nabla_z [y(\sigma_{ix} + \sigma_{jx}) - x(\sigma_{iy} + \sigma_{jy})]. \end{aligned} \tag{A.5}$$

There are three components in A.5. For each component, we calculate the spin part as previously, then use Fourier transformation to calculate the derivatives with proper symmetries. That is how we calculate the Hamiltonian in two-nucleon system. The iteration in Lanczos converges quickly. So this is a good tool to double-check the spin-orbit interactions in auxiliary field diffusion Monte Carlo.